AD NUMBER

AD827679

LIMITATION CHANGES

TO:

Approved for public release; distribution is unlimited.

FROM:

Distribution authorized to U.S. Gov't. agencies and their contractors; Critical Technology; FEB 1968. Other requests shall be referred to Air Force Technical Applications Center, Attn: VELA Seismological Center, Washington, DC 20333. This document contains export-controlled technical data.

AUTHORITY

usaf ltr, 25 jan 1972

LATERAL VARIATIONS IN CRUSTAL STRUCTURE BENEATH THE MONTANA LASA

16 February 1968

Prepared for

AIR FORCE TECHNICAL APPLICATIONS CENTER
Washington, D. C.

By

P. Glover
TELEDYNE, INC.

S. S. Alexander
PENNSYLVANIA STATE UNIVERSITY

Under

Project VELA UNIFORM

Sponsored By

ADVANCED RESEARCH PROJECTS AGENCY
Nuclear Test Detection Office
ARPA Order No. 624

LATERAL VARIATIONS IN CRUSTAL STRUCTURE BENEATH THE MONTANA LASA

SEISMIC DATA LABORATORY REPORT NO. 205

AFTAC Project No.:	VELA T/6702
Project Title:	Seismic Data Laboratory
ARPA Order No.:	624
ARPA Program Code No.:	5810
Name of Contractor:	TELEDYNE, INC.
Contract No.:	F 33657-67-C-1313
Date of Contract:	2 March 1967
Amount of Contract:	$ 1,736,617
Contract Expiration Date:	1 March 1968
Project Manager:	William C. Dean (703) 836-7644

P. O. Box 334, Alexandria, Virginia

This research was supported by the Advanced Research Projects Agency, Nuclear Test Detection Office, under Project VELA-UNIFORM and accomplished under the technical direction of the Air Force Technical Applications Center under Contract F 33657-67-C-1313.

ABSTRACT

The analysis of a variety of geologic and geophysical data indicates that significant lateral variations in crustal structure exist across LASA. This structural complexity is inferred from observation of Rayleigh wave dispersion, body-wave spectral ratios, P-wave amplitude and travel-time anomalies, seismic refraction profiles and gravity and magnetic anomalies. To explain these results, LASA is divided into an eastern and a western sector. An attempt is made to explain the observations in each sector in terms of crustal models consisting of 3 to 5 distinct layers. The observations show that the maximum lateral change in structure across LASA takes place in a NE-SW direction.

ACKNOWLEDGEMENTS

We are grateful to Dr. Louis Pakiser and Mr. Isidore Zeitz of the Office of Earthquake Research and Crustal Studies, U.S. Geological Survey, Menlo Park, California for making available to the authors copies of the gravity and aeromagnetic maps of the LASA area in advance of publication.

TABLE OF CONTENTS

LIST OF FIGURES

LIST OF TABLES

INTRODUCTION

This report summarizes the results of a study to determine the structure of the earth's crust beneath the Large Aperture Seismic Array (LASA) in Montana, from available geological and geophysical data. The array is composed of 525 short-period vertical-component seismometers grouped into 21 subarrays each with 25 sensors. In addition, three-component long-period seismometers are located at the center of each subarray (Figure 1).

In order first to establish the geologic setting of the array we review briefly all data available at this time and introduce some new evidence. Both surface measurements and well-log data provide stratigraphic evidence for lateral variation in crustal structure under the array; however these data pertain only to the uppermost three kilometers.

Several seismic refraction studies relevant to the deeper structure have been conducted in Montana over the past decade. The results obtained prior to 1964 have been summarized by McCamay and Meyer (1964) and James and Steinhart (1966). A more recent study (1966) has been conducted by the U.S. Geological Survey (Borcherdt and Roller, 1967). Crustal models based on those refraction profiles which pass through the array provide starting points for the present interpretation of LASA structure.

Fundamental mode Rayleigh wave phase and group velocity dispersion curves, computed for the array as a whole and for a number of individual sectors using two teleseismic events known to have high signal-to-noise ratios, yield additional evidence on LASA structure. A comparison of these data with theoretical dispersion curves for three proposed crustal models based on the seismic refraction studies, calculated using a computer program developed by Harkrider and Anderson (1962), provides a quantitative measure of the lateral variation in structure across the array. In addition curves showing phase propagation direction for both events as a function of period, for the whole array and for individual sectors, allow us to infer the orientation of major structural trends.

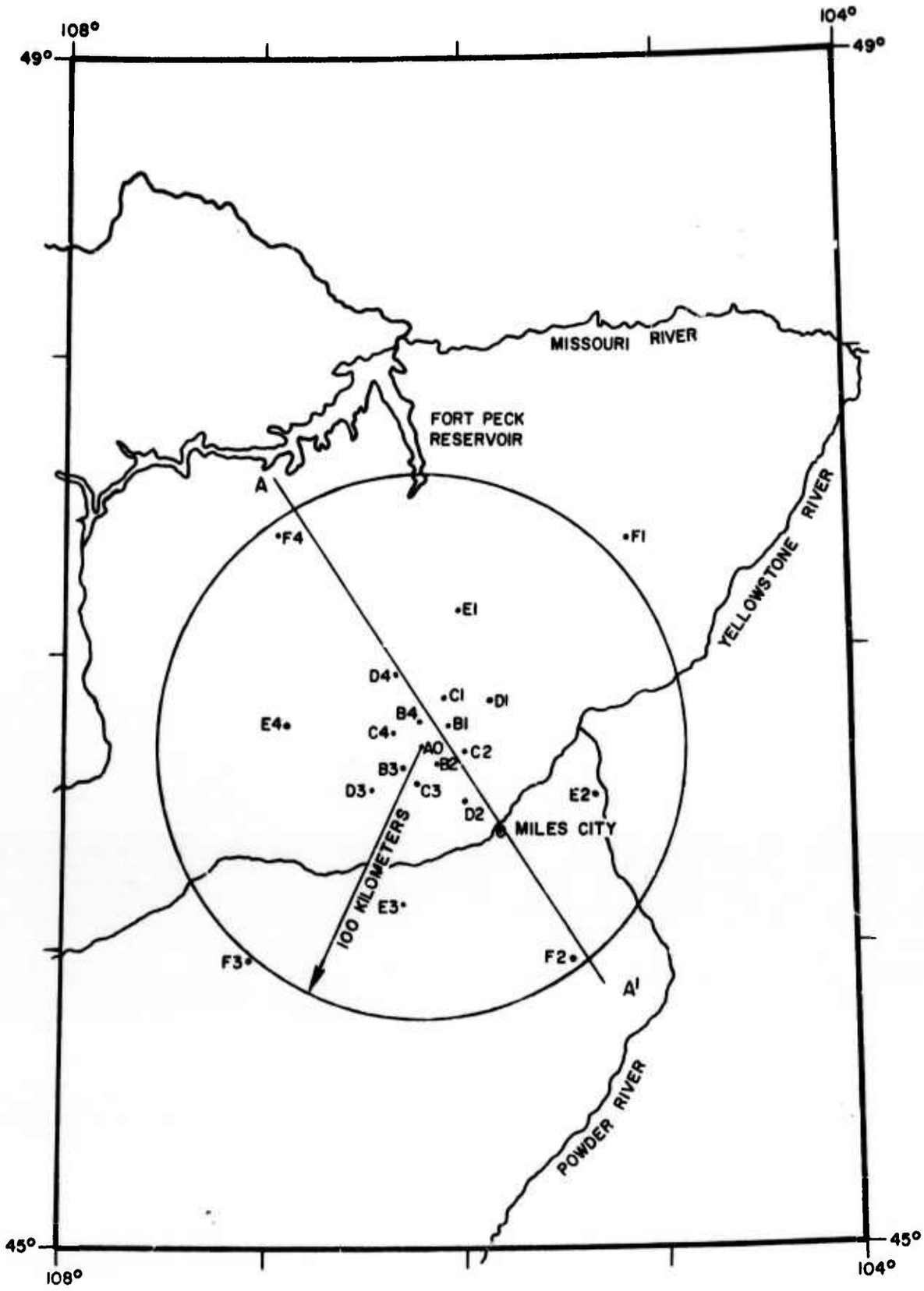

Figure 1. Location of the Montana LASA

Long-period body-wave spectral ratios calculated at each of the subarrays for two events well recorded at LASA further indicate variations in the crustal transfer function across the array. Phinney (1964) has demonstrated that these ratios are diagnostic of the crustal structure beneath the receiving station and that in certain cases such data may be inverted to deduce an approximate structure. In the present study the observed spectral ratios are compared with theoretical ratios calculated for the refraction models, and we attempt to use the observed spectral ratios to define systematic variations in structure across the array.

Sheppard (1967) studied travel-time anomalies at LASA for short-period P-waves and found that these defined a region of low velocity in the form of a NE plunging syncline with its axis somewhat to the north of the center of the array. We compare the travel-time anomalies at LASA given by Chiburis (1966) for several seismic source regions with those obtained by Sheppard. In addition, we attempt to correlate short-period P-wave amplitude anomalies at LASA with the travel-time anomalies and to determine the dependence of these amplitude anomalies on azimuth of approach.

An unpublished aeromagnetic map of the earth's field in the vicinity of LASA (Zeitz, personal communication, 1967) together with an unpublished Bouguer anomaly map (Pakiser, personal communication, 1967) furnish additional evidence for lateral variation in structure under the array.

Collectively the data support the premise that any important lateral variation of the crust beneath the array is within the basement, for although there is evidence for minor changes of sediment thickness across the array, this alone is insufficient to account for the geophysical observations. It appears that the major tectonic trend in the crust is NW-SE, possibly with a subordinate trend NE-SW.

In the following sections we shall demonstrate that the structure of the earth's crust beneath LASA is considerably more complex than has been previously indicated. Additional detailed work will be needed, however, to account for this complexity in terms of accurate station corrections.

OBSERVATIONAL EVIDENCE CONCERNING LASA STRUCTURE

Geologic Evidence

Geologic cross sections through the array (Brown and Poort, 1965; Anon, 1965) show that the sedimentary sequence under LASA consists of nearly horizontal layers. Table 1 gives a summary of their lithology, thickness, trend of known tectonic features and the corresponding P-wave velocities given by Brown and Poort. The maximum thickness of sediments reported is 11,414 feet from Stanolind bore-hole NPRR #1-E which is located some 10 km to the NE of subarray F1. This hole bottoms out in Ordovician rocks; hence it is unlikely that the total sedimentary sequence greatly exceeds the 3.2 km given by Brown and Poort. There is no evidence of a major lateral discontinuity or abrupt change in lithology to these depths with the exception of the uppermost 500 feet where rapid facies changes are common (Anon, 1965).

The structural contour map (Figure 2), based on surface measurements with good control from existing well data, shows the depth to the base of the Colorado Shale. This map indicates that the post-Lower Cretaceous sediments thicken eastward by approximately 2500 feet across the array from the Procupine Dome in the west toward the western margin of the Williston Basin to the east of the array. This thickening does not, however, define a clearly synclinal structure, but rather it is a downwarping with a NW-SE strike truncated at the eastern margin of the array by the Cedar Creek Anticline. The pre-Cretaceous rocks thin over the Miles City Arch which lies to the south of subarray A0. They tend to thicken towards the NE from the Porcupine Dome, a feature which protrudes prominently into the sedimentary section. In addition to the NW-SE structural trend, these rocks bear evidence of an earlier episode of folding with a NE-SW trend.

These geologic data, then, indicate that should any radical lateral change take place it must do so within the basement (i.e., at a depth greater than 3 km). Furthermore, the tectonic setting of LASA indicates that such a discontinuity would likely have a NW-SE trend. The possibility of transcurrent faulting in an E-W direction to the west of LASA

Table 1. Description of Stratigraphic Sequency Beneath the Montana LASA.

AGE	DESCRIPTION	AVERAGE THICKNESS (km)	P-WAVE VELOCITY (km/sec)
TERTIARY-CRETACEOUS	Sandstones and shales. conformably on Lower Cretaceous rocks; dips less than 1/2°, increasing slightly over Porcupine Dome.	1.2	3.0
L. CRETACEOUS-JURASSIC	Essentially sandstones and shales. Dips less than 2°, towards the N.E. Structural features trend NW-SE.	0.5	3.8
PALEOZOIC	Predominately limestone and dolomite. Thickness variable; thinnest over Porcupine Dome and Miles City Arch. Beds essentially horizontal. Structures, where present, trend NW-SE, with evidence of a pre-Cretaceous NE-SW structural trend. Off-lap of some horizons over the arch.	1.3	5.8
PRE-CAMBRIAN	Metamorphic rocks. Granites and gneisses. Steeply inclined with NW-SE structural trend, and remnant Paleozoic NE-SW structre.	>6.5	?

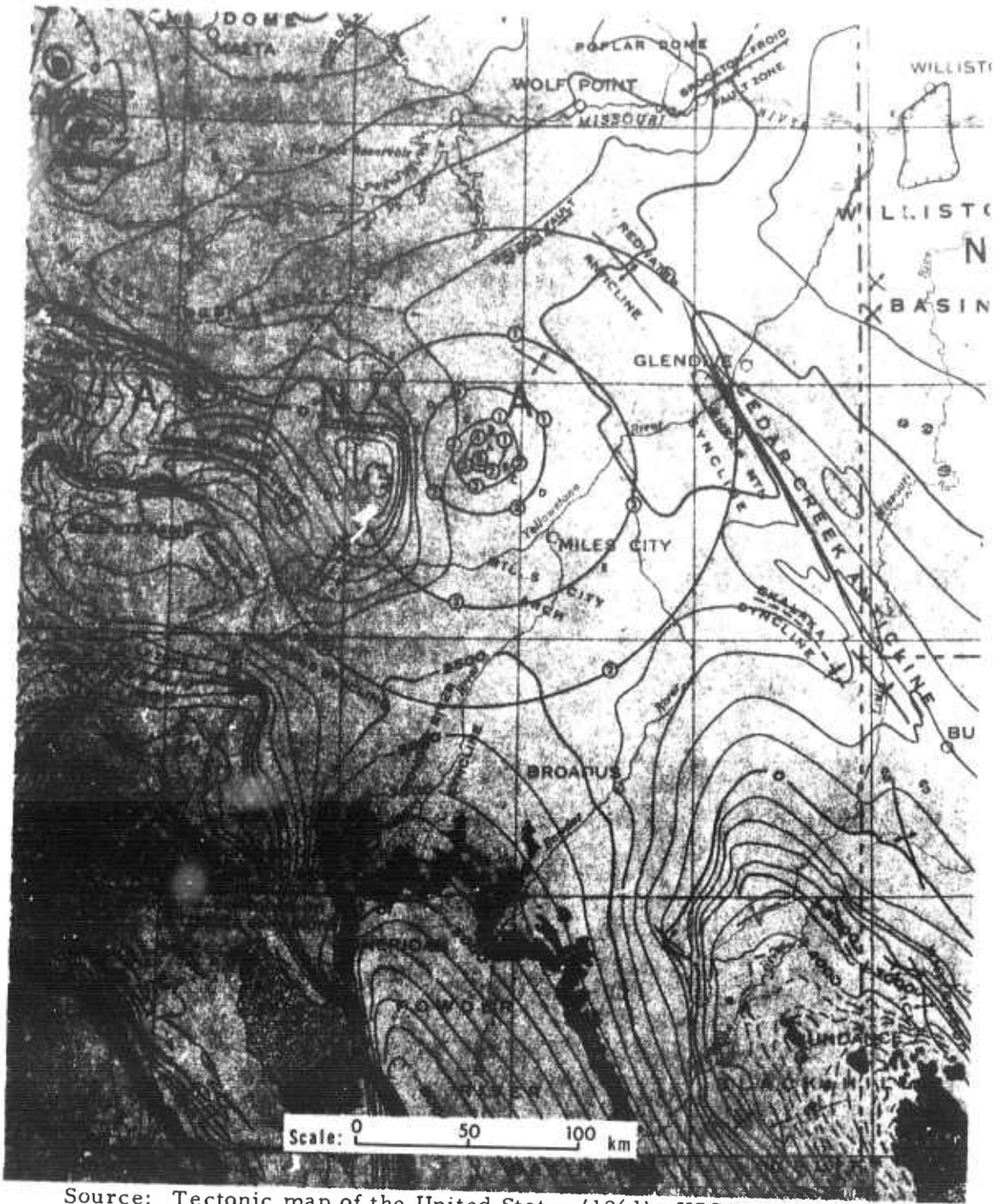

Source: Tectonic map of the United States (1961), USGS and AAPG

Figure 2. Tectonic Setting of LASA

has been suggested (Smith, 1965); however, there is no conclusive evidence to support the extension of these postulated faults into the area covered by LASA.

Thus the available geological data for LASA pertain directly to only the uppermost 3 km of the earth's crust. For the deeper structure we must rely solely on geophysical data.

Seismic Evidence

Seismic Refraction Data

Seismic refraction studies in Montana have been conducted by the University of Wisconsin (Meyer, et al, 1961), the Carnegie Institution of Washington (Aldrich and Tuve, 1960; summarized in McCamay and Meyer, 1964, and James and Steinhart, 1966; Asada and Aldrich, 1966) and more recently by the U.S. Geological Survey (Borcherdt and Roller, 1967). Figure 3 shows the location of all these available profiles within the LASA area.

The model given by Meyer, et al. (1961) for a N-S profile passing through the array is shown in Figure 4, along with a model for a N-S profile within the Rocky Mountains to the west of LASA. Comparison of the two models shows that the crustal structure in Montana is complex and suggests that the base of the crust not only decreases in depth westward between the two profiles, but also changes its direction of dip from northerly in the east to southerly in the west. However, the Carnegie results, for unreversed profiles (Asada and Aldrich, 1966), and the University of Wisconsin results from profiles perpendicular to those shown in Figure 4 show little overall agreement. A horizontal-layer approximation to the model for the reversed N-S profile across LASA given by Meyer, et al. (1961) forms the basis for model U.W.3 in Table 2.

According to James and Steinhart (1966) the most significant conclusion to be drawn from refraction work in this region is that the crust under the Northern Rocky Mountains is thinner than that beneath the Great Plains to the east; typical crustal thicknesses for the Northern Rocky Mountains are 35-45 km, and those for the Great Plains are around 45-55 km.

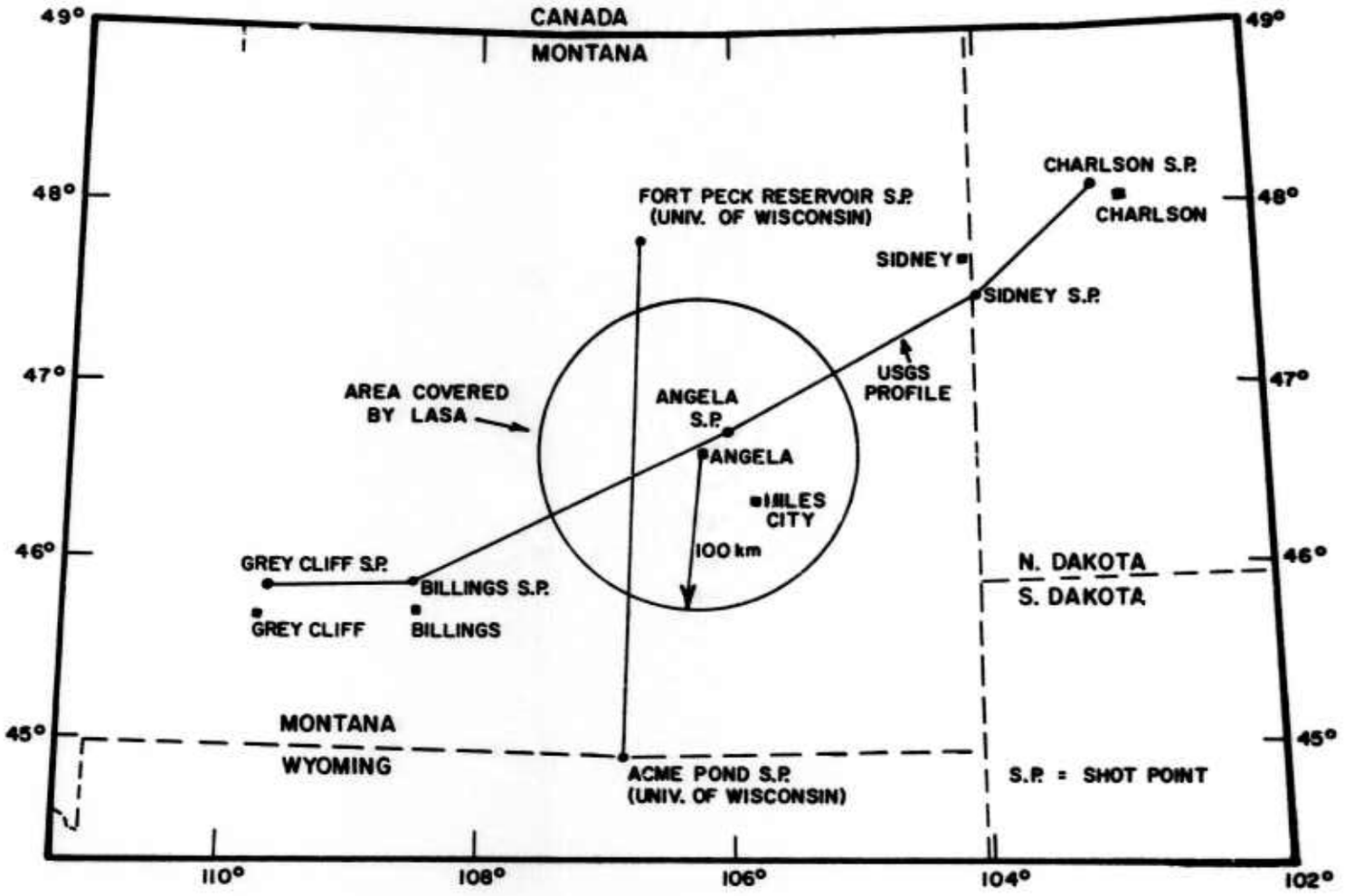

Figure 3. Location of Seismic Refraction Profiles through LASA. (After Borcherdt and Roller 1967).

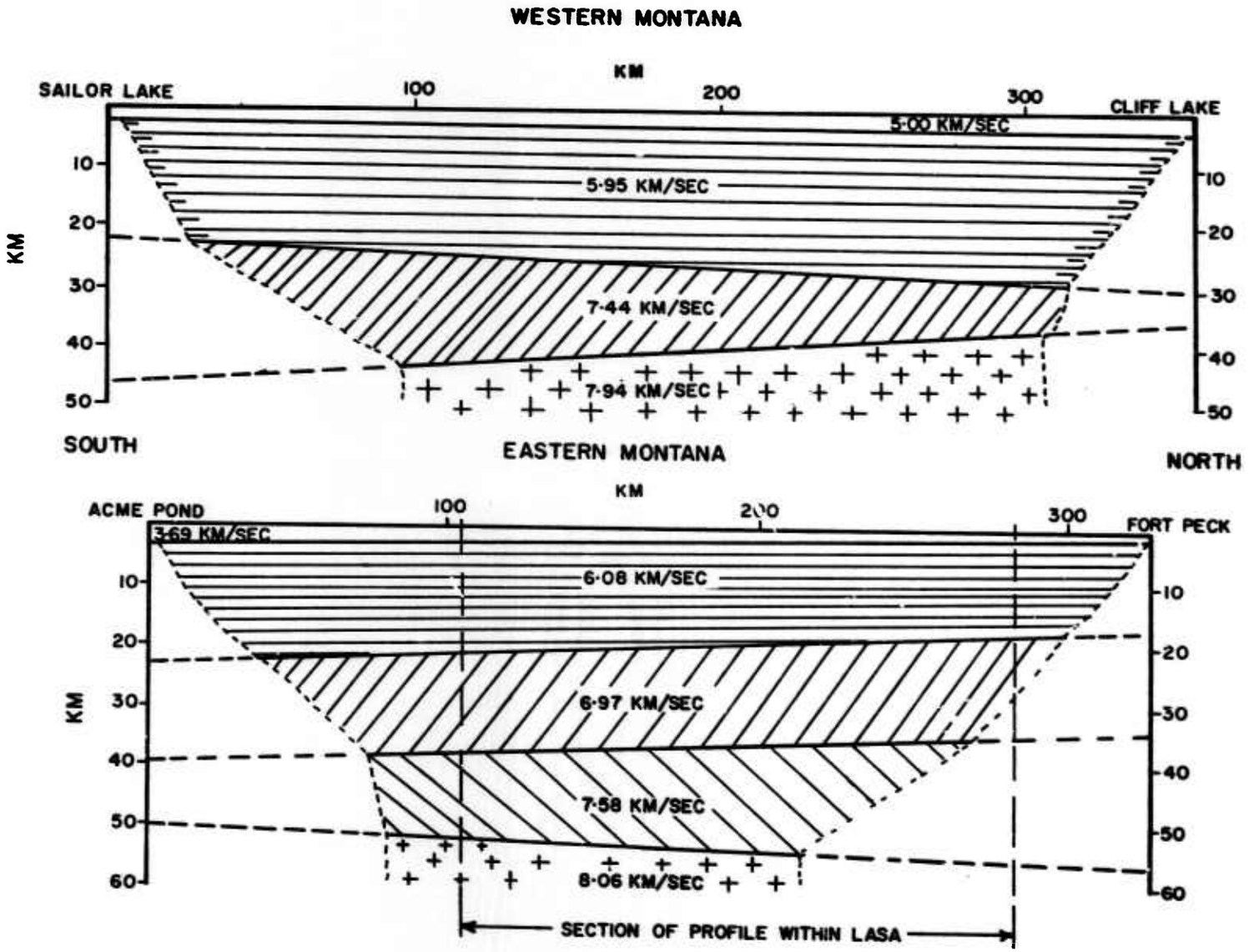

Figure 4. The University of Wisconsin Crustal Models.
(After Meyer et al, 1961)

Table 2. Parameters of the LASA Crustal Models based on Seismic Refraction Studies.

MODEL	LAYER PARAMETERS			
	P-wave velocity km/sec	S-wave velocity km/sec	Density gm/cc	Thickness km
U.W.3	2.60	1.48	2.31	0.3
	3.70	2.16	2.54	2.5
	6.08	3.61	2.85	17.5
	6.97	4.06	3.10	17.0
	7.58	4.36	3.22	16.5
	8.07	4.65	3.55	+*
USGS3	3.00	1.77	2.40	2.5
	6.15	3.61	2.90	19.5
	6.70	3.96	3.02	27.0
	8.30	4.60	3.65	+*
T.I.1	2.60	1.50	2.31	0.3
	3.70	1.85	2.54	2.0
	6.08	3.51	2.85	15.0
	6.97	4.11	3.10	17.0
	7.58	4.47	3.22	23.0
	8.07	4.67	3.55	+*

*+ denotes half-space

The model obtained by the USGS (Borcherdt and Roller, 1967) is shown in Figure 5 and the horizontal-layer approximation, which forms the basis for the model USGS3, is given in Table 2. This model agrees with the conclusions of James and Steinhart (1966) in that it shows a gradual thinning of the crust westwards. Three important differences in this model compared to the model U.W.3 are:

1. the number of layers within the basement (two vs. three for U.W.3)

2. The lower average P-wave velocity for the crust (6.1 km/sec vs. 6.5 km/sec)

3. the higher mantle velocity (8.3 km/sec vs. 8.07 km/sec)

In both models the shear-wave velocity was calculated using values of Poisson's ratio appropriate to the model CANSD given by Brune and Dorman (1963) for the Canadian Shield. The third model, T.I.1, is a model given by Miller, et al., (1967) also based on the University of Wisconsin work. It differs from the U.W.3 model in its shear-wave velocities, as can be seen from Table 2. Densities for all models were found using empirical data quoted by Steinhart and Woollard (1961) which gives density as a function of compressional-wave velocity.

These refraction data suggest that the crust is somewhat thinner under the western sector of LASA. However, the layers within the crust are not uniformly dipping, so that there results a net reduction in average crustal velocities toward the SW across the array. This can be seen by comparing Figures 4 and 5 and noting the corresponding locations in Figure 3. This SW decrease in average crustal velocity is supported by the surface-wave dispersion observations to be discussed below.

Rayleigh Wave Dispersion Data

The two events used in this study for dispersion measurements occurred on November 18, 1966, one in the Greenland Sea and the other on the North Atlantic Ridge. Table 3 gives the

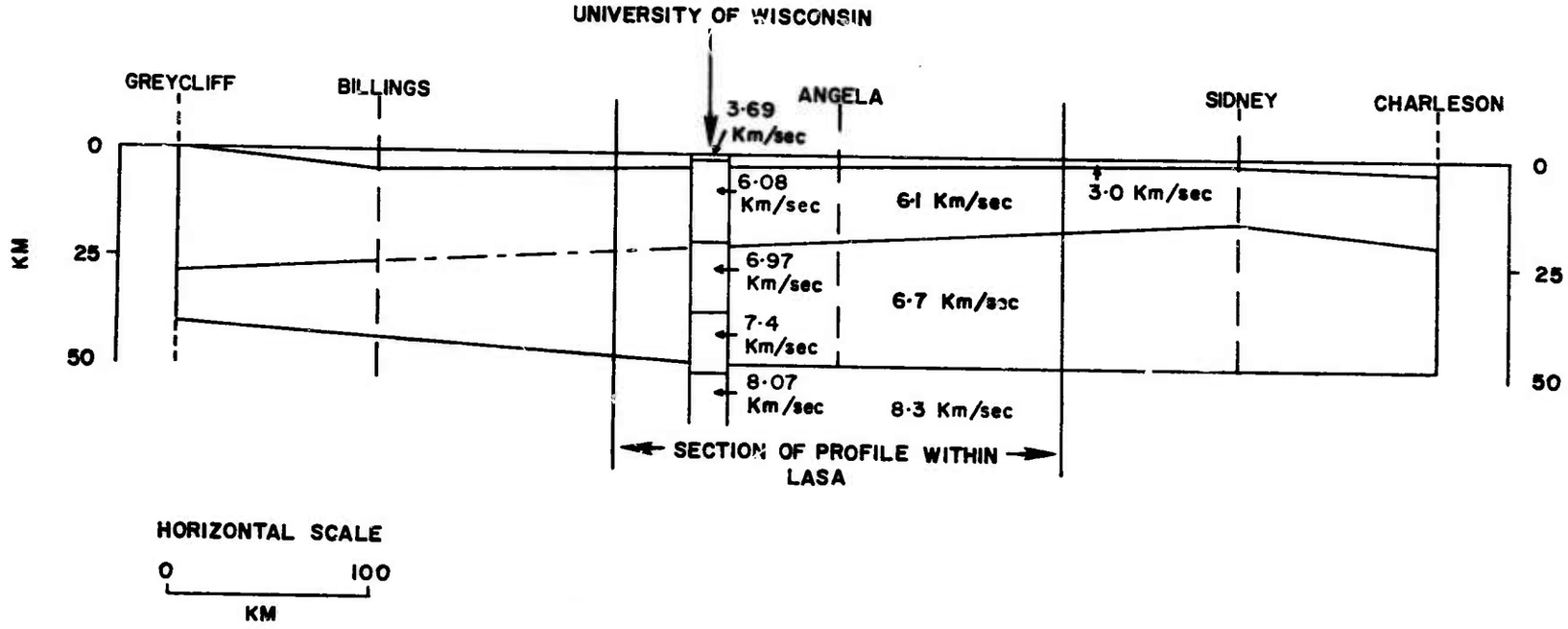

Figure 5. The USGS Crustal Model. (After Borcherdt and Roller, 1967)

TABLE 3. Epicenter Data for Events used in Rayleigh Wave Dispersion Studies

DATE:	18 November, 1966	18 November, 1966
ORIGIN TIME:	18:48:43.9	07:08:30.0
AREA:	Greenland Sea	N. Atlantic Ridge
LATTITUDE:	73.4 N	32.2 N
LONGITUDE:	6.8 E	40.5 W
DEPTH:	33 km	33 km
MAGNITUDE:	4.9 c.g.s.*	4.5 c.g.s*

*body wave magnitudes as given by USC&GS

epicenter data for these events. LASA long-period vertical component seismograms for both events (see Figure 6) show a well-dispersed fundamental mode Rayleigh wavetrain with a mean signal-to-noise ratio of 47 for the Greenland Sea event and 42 for the North Atlantic Ridge event; signal-to-noise ratio here is defined as the maximum (zero-to-peak) amplitude of the signal divided by the rms amplitude of the noise proceeding the signal. No beats were observed at any of the twenty one subarrays, indicating that there were no prominent multiple path arrivals. Examination of the signal spectra for each station revealed no pronounced minima within the period range considered. (For typical examples, see Figure 7). From the digital records, a time interval corresponding to a group velocity window from 4.0 to 2.8 km/sec was selected.

All calculations of dispersion and direction of propagation were made in the frequency domain using the numerical Fourier transforms of the long-period vertical-component seismograms. The details of these computational procedures are given in Appendix I.

Figure 8 presents the observed phase and group velocity dispersion data for the Greenland Sea event. Curves are shown for the whole array and the eastern and western sectors divided by a line (A-A' in Figure 1) trending N20°W through Miles City. The eastern sector consists of the subarrays F1, E1, E2, D1, C1, C2, and B1; the western sector, F2, F3, F4, E3, E4, D2, D3, D4, C3, C4, B2, B3, B4, and A0. This division separates the array into two regions which, from aeromagnetic data (discussed below), appear to have contrasting magnetic properties (Zeitz, personal communication, 1967). Figure 9 presents similar data for the North Atlantic Ridge event. Corresponding phase propagation directions as a function of period for these events and sectors are shown in Figures 10 and 11. For both events, the phase velocities in the eastern sector are somewhat higher than those for the array as a whole, with the exception of those corresponding to period of 15-23 seconds from the North Atlantic Ridge event, which are slightly lower. Observed phase velocities in the western sector are lower than those for the whole array at all periods in the range 15 to 60 seconds. This implies either that the deeper layers of the crust to the

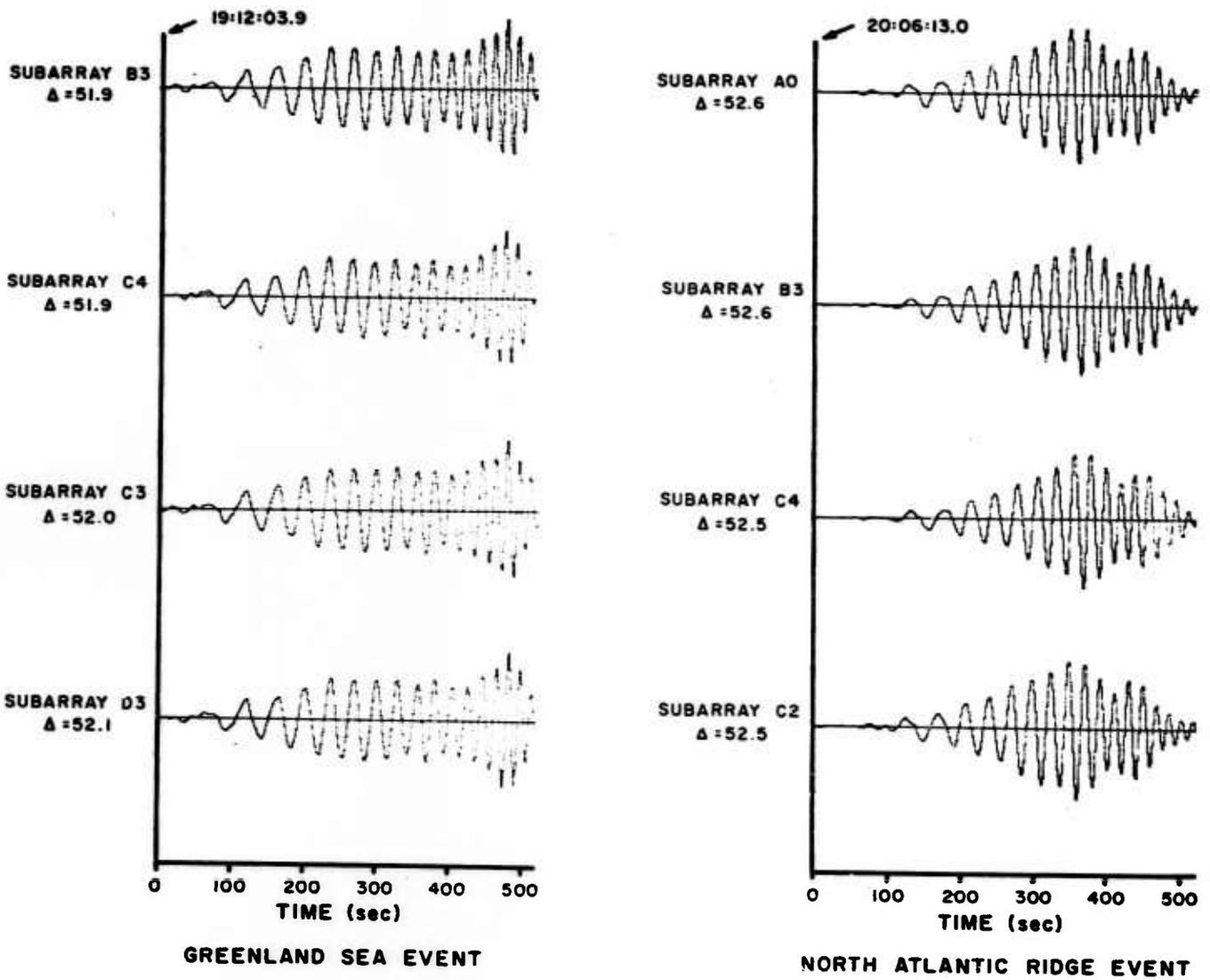

Figure 6. Typical Long-period Vertical-component Seismograms Recorded at LASA from the Greenland Sea and North Atlantic Ridge Events

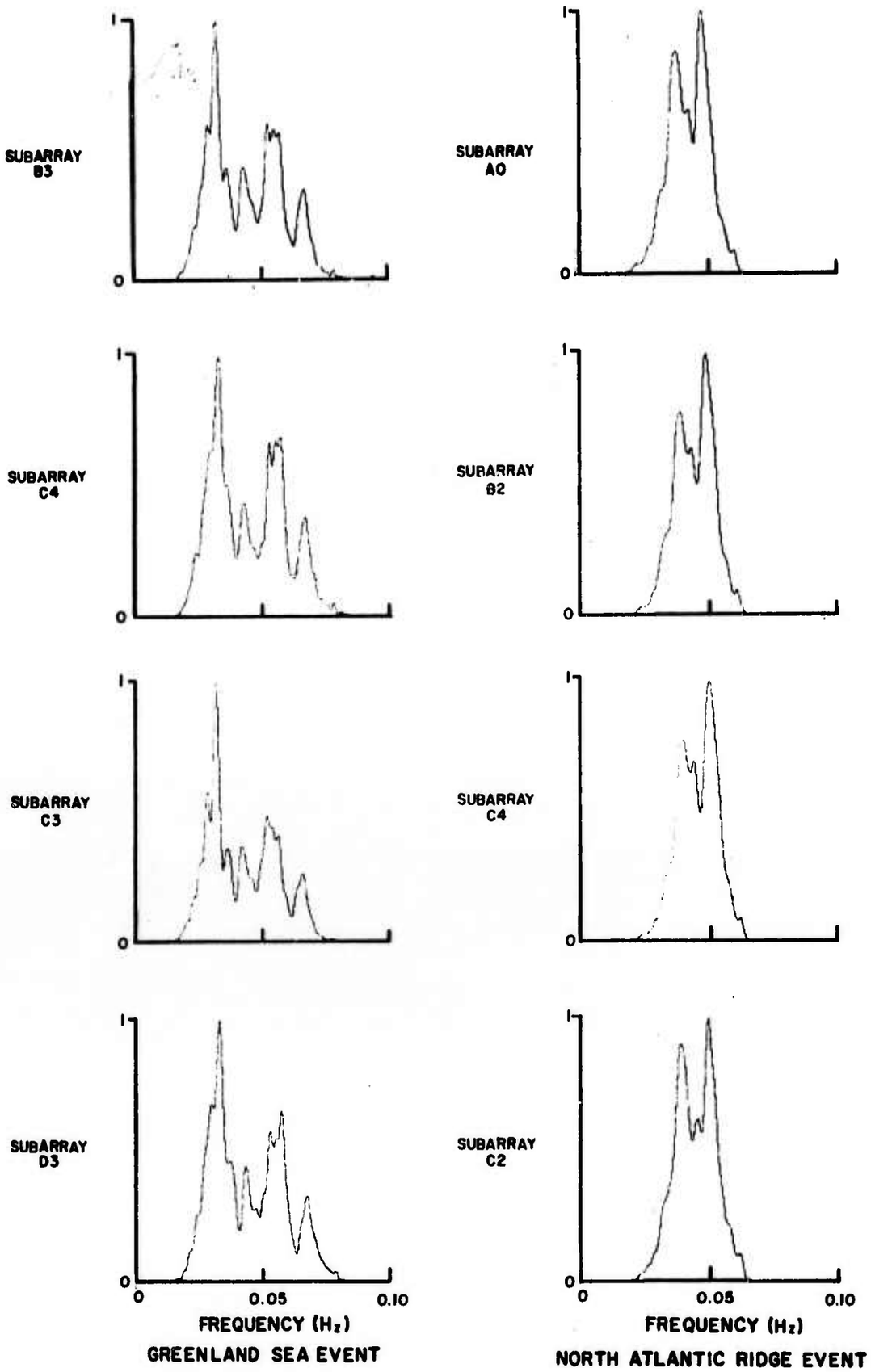

Figure 7. Normalized Power Spectra of the Seismograms shown in Figure 6

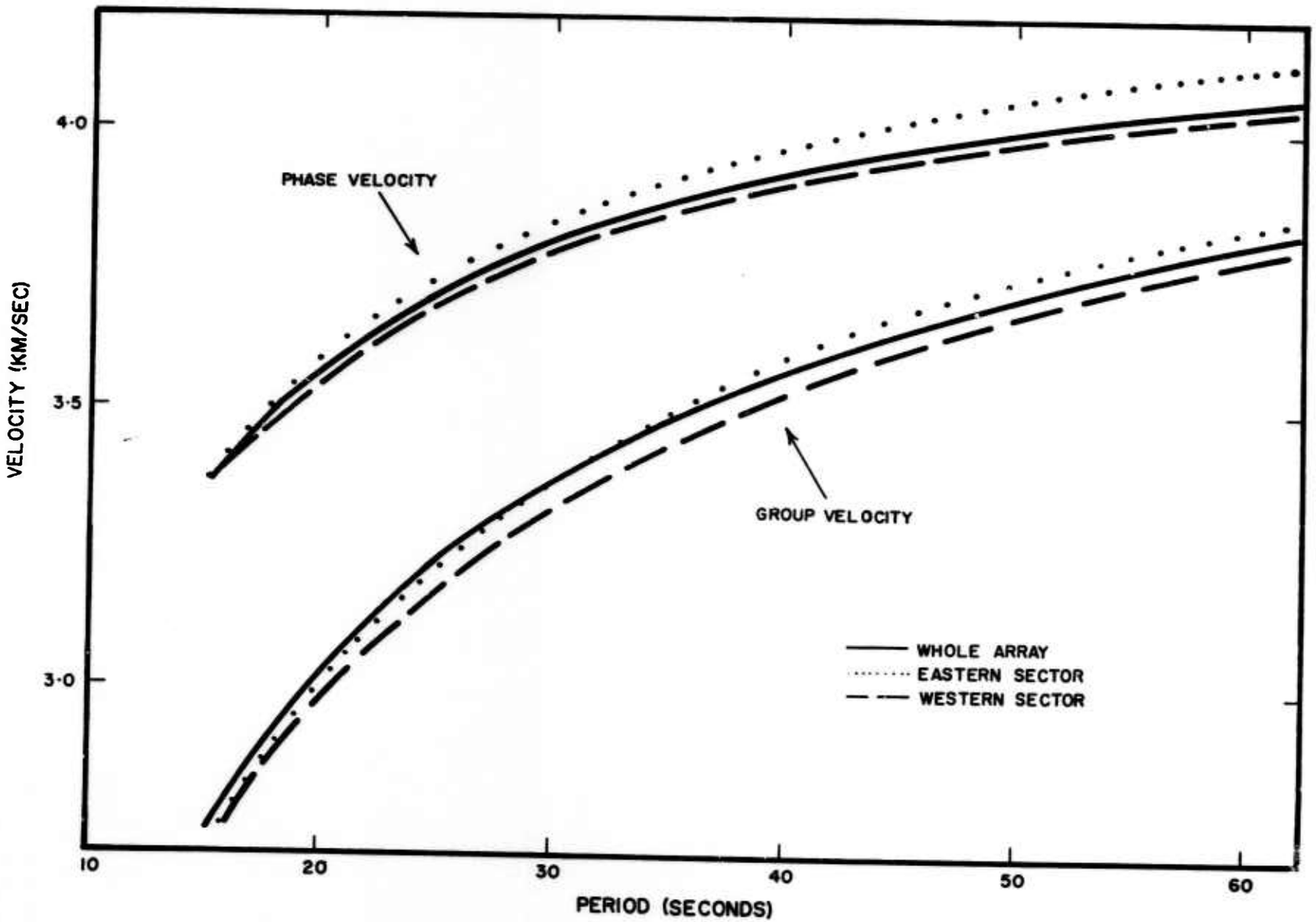

Figure 8. Observed Rayleigh Wave Dispersion for the Greenland Sea Event

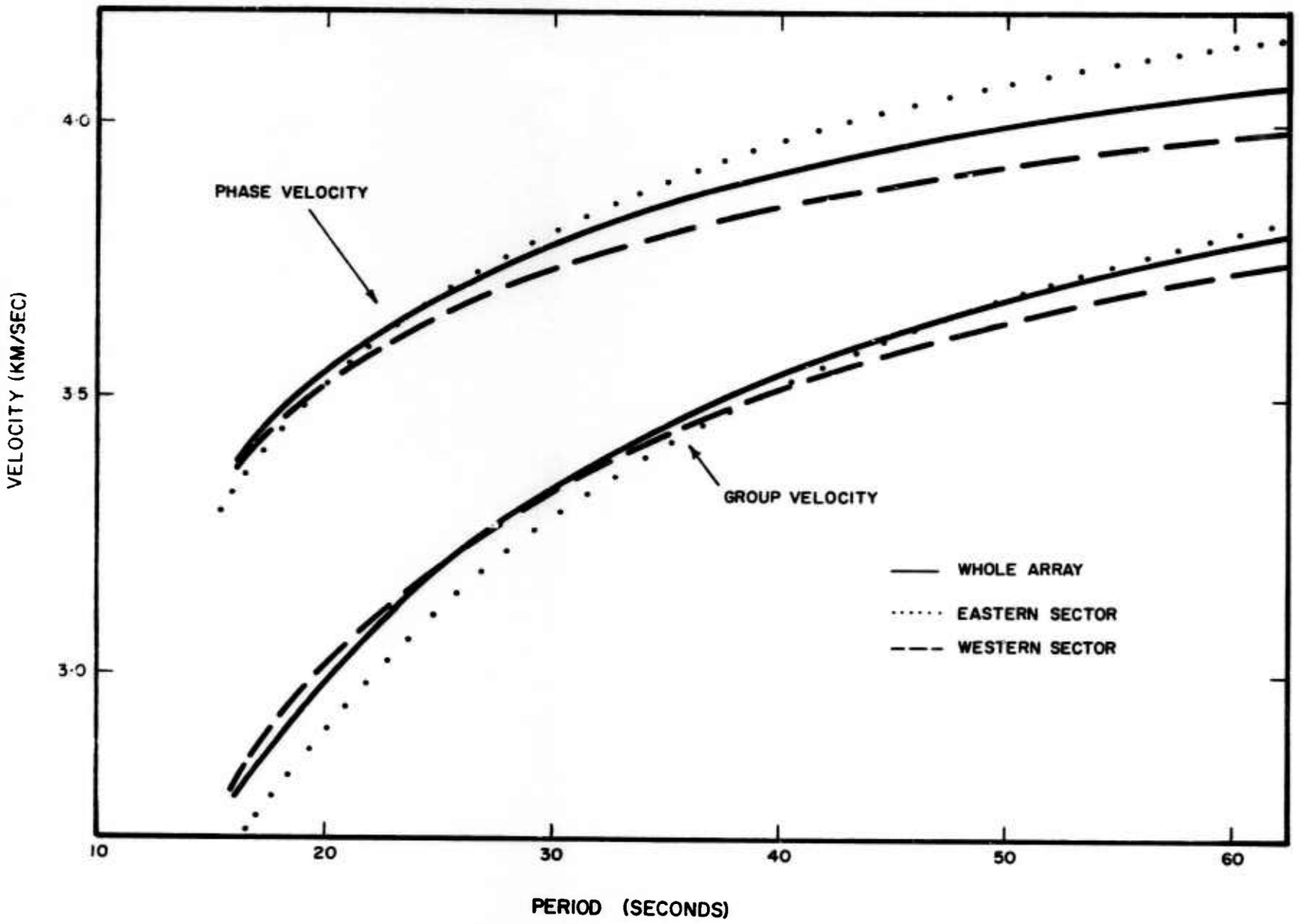

Figure 9. Observed Rayleigh Wave Dispersion for the North Atlantic Ridge Event

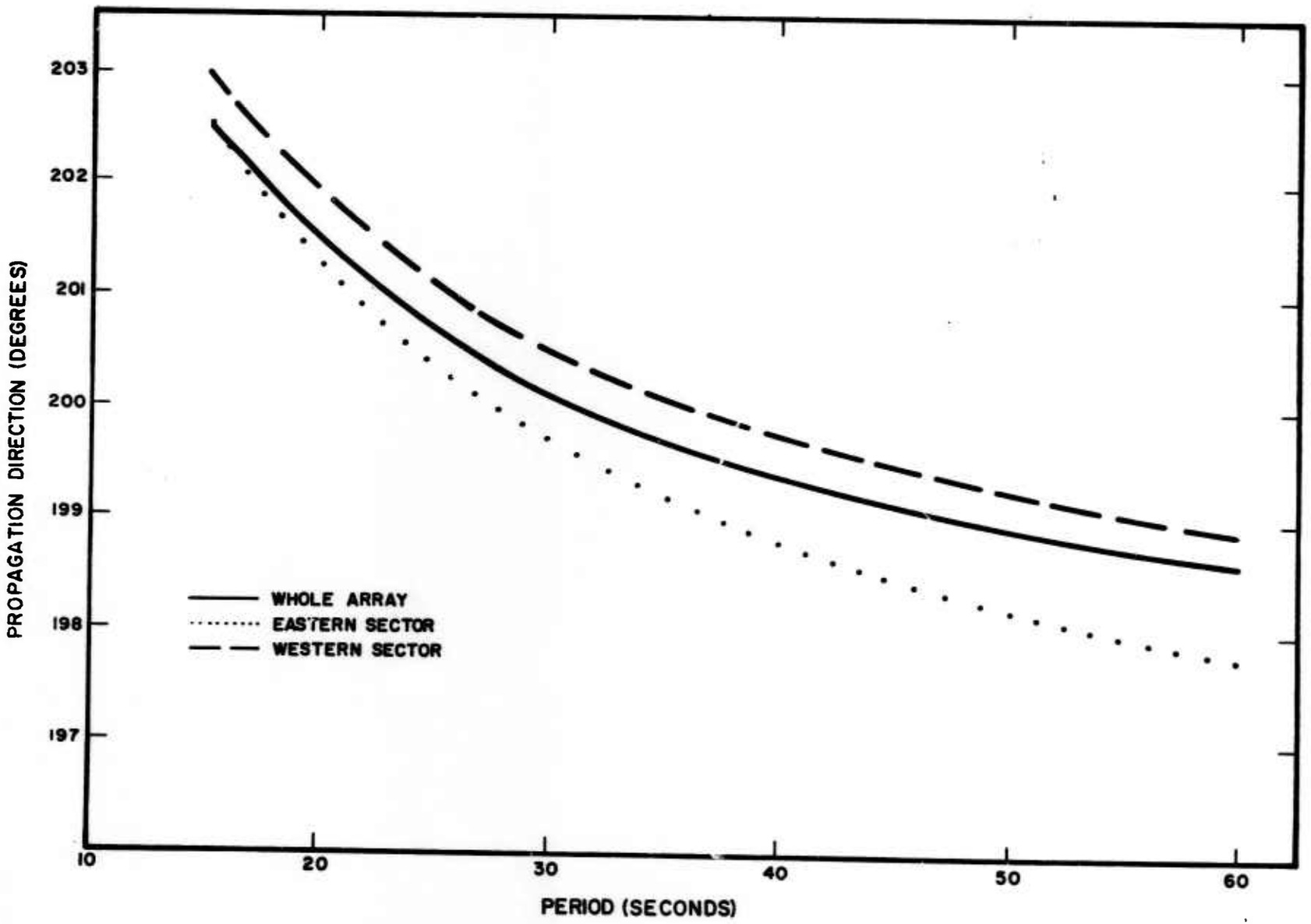

Figure 10. Observed Phase Propagation Directions for the Greenland Sea Event

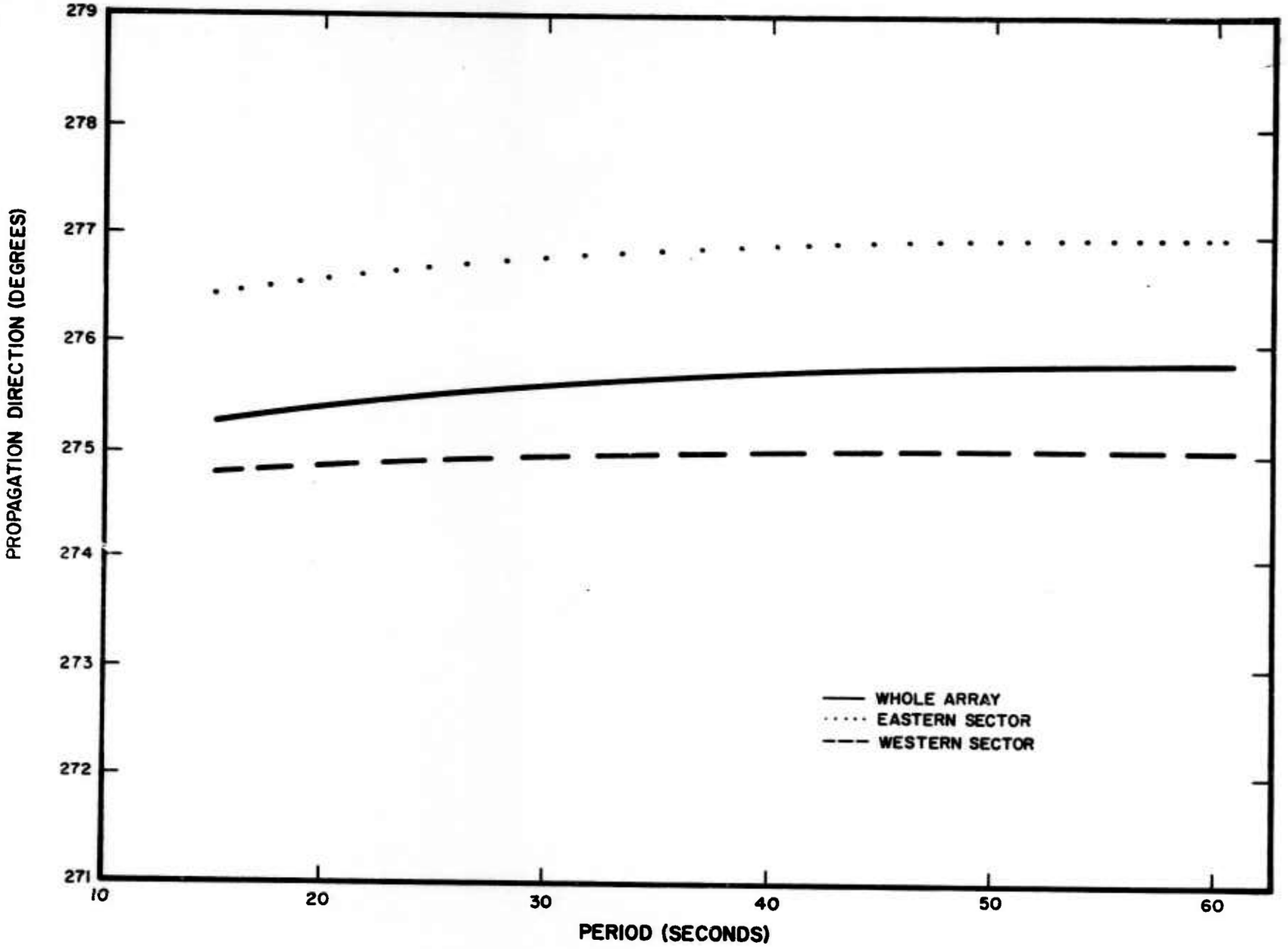

Figure 11. Observed Phase Propagation Directions for the North Atlantic Ridge Event

west are thicker, or that the velocities decrease to the west, or both. The shallower part of the structure apparently does not change as markedly laterally, since the phase velocity variations are small for the two events and both sectors at the shorter periods. This result is consistent with the geological evidence for the uppermost three km discussed earlier.

For a given period, the direction of propagation systematically increases in azimuth from east to west across the array for the Greenland Sea event, whereas for the North Atlantic Ridge event which has a more southerly back-azimuth to the source, the propagation directions systematically decrease in azimuth. This indicates a lateral change in structure occurs with a trend whose normal lies between the back-azimuths of the two events (i.e., the structural trend lies between N70°W and N5°E). Since the surface waves are refracted towards the normal on crossing the boundary between the eastern and western sectors of the array, phase velocities must be lower in the western sector. This agrees with the actual measured phase velocities for these sectors, as mentioned above. It is possible to use this measured change in direction of propagation to determine the strike of the structural feature giving rise to the lateral refraction. The method for making this determination is outlined in Appendix II.

Figure 12 is a plot of the change in propagation direction $\beta_i(T)$ versus $\alpha_i(T)$, the direction of propagation in the eastern sector, for the Greenland Sea and North Atlantic Ridge events. The value of $\alpha_i(T)$ at $\beta_i(T) = 0$, denoted by $\alpha_o(T)$, gives the direction normal to the structural trend (See Appendix II). Since there are but two points to determine each curve, only a lower bound can be placed on α_o. The results are significant in that they show that the average strike of the boundary is northwest and less than N54°W for all periods considered. The variation of α_o with period suggests that the strike of the boundary becomes more nearly N-S in the shallower part of the crust. It should be pointed out, however, that this result does not imply anything about the sharpness of the boundary separating the two sectors, only that a structural trend in the indicated direction exists.

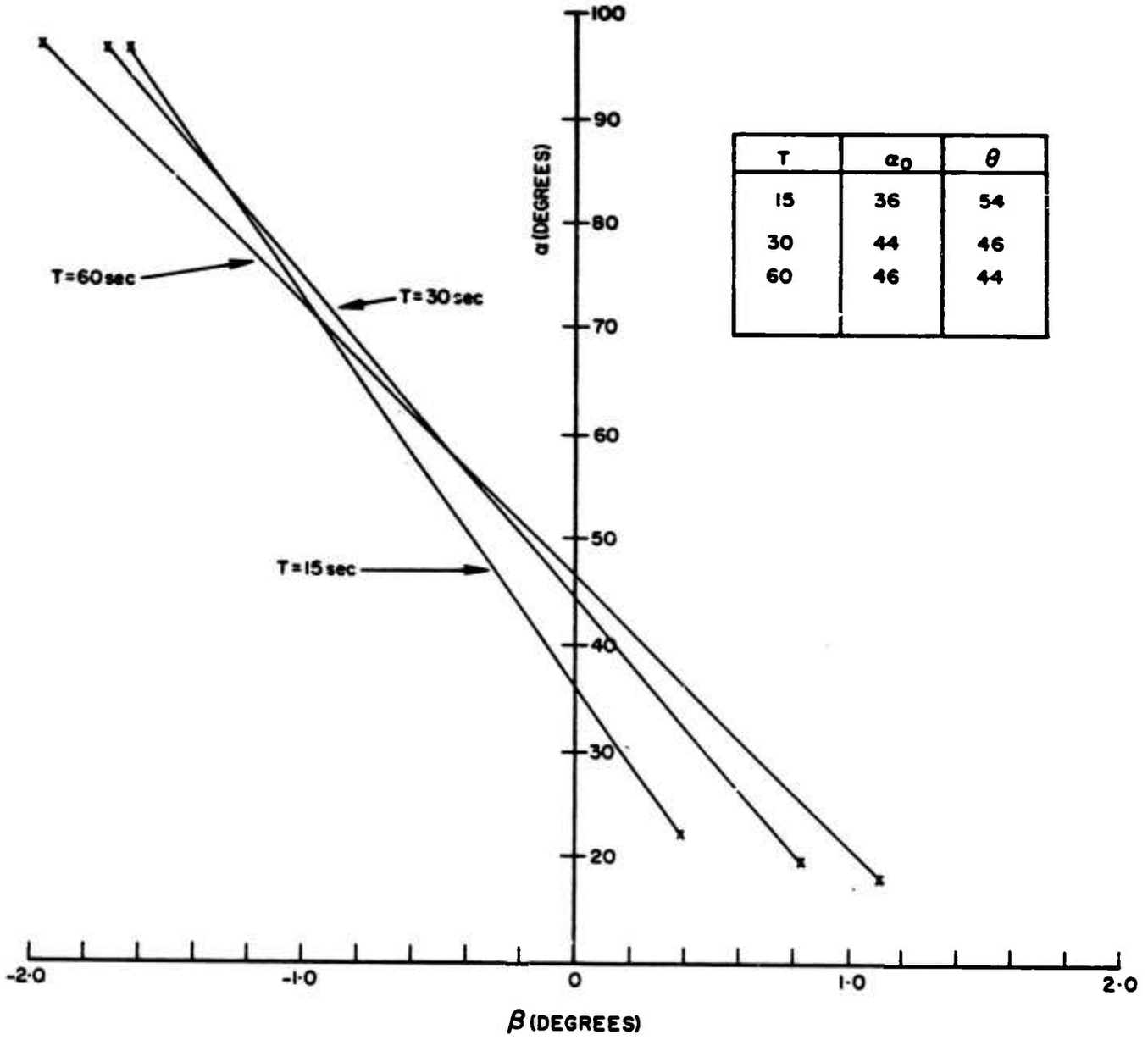

T	α_0	θ
15	36	54
30	44	46
60	46	44

Figure 12. Curves showing Change in Propagation Direction across LASA as a Function of Back-Azimuth to the Apparent Source for the Greenland Sea and North Atlantic Ridge Events

The group velocity dispersion curves also show higher velocities in the eastern sector than in the western one. Since the reliability of these curves is questionable because of the manner in which they were computed (See Appendix I) we will not attempt to interpret them, although they are generally consistent for the two events analyzed.

Dispersion curves were also obtained for the Greenland Sea event for a northern sector of the array consisting of the subarrays F1, F4, E1, E4, D1, D4, C1, C4, B1, B4 and a southern sector of F2, F3, E2, E3, D2, D3,C2, C3, B2, and B3. This division was suggested by Sheppard's (1967) interpretation of short period P-wave travel-time anomalies at LASA. The phase velocities in the north were found to be somewhat higher than those for the south (See Table 4) but very nearly equal to those for the whole array. The phase velocities for the southern sector were somewhat lower than for the whole array. The contrast in phase velocities between the northern and southern sectors is considerably less than the contrast between the eastern and western sectors. This indicates that the N20^{o}W trending line between the eastern and western sectors (A-A' in Figure 1) better divides LASA into distinct regions than does the division into northern and southern sectors.

Phase velocities were also determined for an outer group consisting of subarrays F1, F2, F3, F6, E2, E4, and an inner group A0, B1, B2, B3, B4, C1, C2, C3, C4, D1, D2, D3, and D4, using the Greenland Sea event. This division was made primarily to test whether or not LASA appears as a structural basin. In this case, the velocities for the two sections are essentially equal and almost identical with those for the array as a whole (Table 4). This suggests that the array is not a structural basin.

Collectively, the Rayleigh wave dispersion data indicate that a lateral change in crustal structure takes place across LASA. The maximum change takes place perpendicular to a line trending NW through Miles City, Montana. This line (A-A' in Figure 1) divides the array into an eastern sector composed of the subarrays F1, E1, E2, D1, C1, C2, and B1 and a western sector consisting of F2, F3, F4, E3, E4, D2, D3, D4, C3, C4, B2, B3, B4, and A0. For both events analyzed, the observed

Table 4. Phase Velocities for the Greenland Sea Event

PERIOD	PHASE VELOCITY (km/sec)				
(Seconds)	WHOLE ARRAY	N. SECTOR	S. SECTOR	INNER GROUP	OUTER GROUP
60	4.06	4.07	4.00	4.06	4.07
55	4.03	4.04	3.98	4.03	4.04
50	4.00	4.01	3.96	4.00	4.01
45	3.97	3.98	3.93	3.97	3.98
40	3.93	3.93	3.89	3.93	3.93
35	3.87	3.87	3.84	3.88	3.88
30	3.80	3.80	3.77	3.81	3.80
25	3.70	3.70	3.68	3.71	3.70
20	3.57	3.56	3.56	3.59	3.57
15	3.36	3.35	3.36	3.37	3.34

phase velocities from the eastern sector were higher than those from the western sector of the array. Phase propagation directions also differ systematically between the two sectors.

The division of LASA into a northern and a southern sector yielded observed phase velocities that were inconsistent with Sheppard's (1967) hypothesis that the observed distribution of travel-time anomalies is due to an increase in total crustal thickness of 10 km beneath subarray B4 (with respect to subarrays F4 and F2).

Theoretical dispersion curves for various crustal models were calculated using a computer program developed by Harkrider and Anderson (1962) which computes phase and group velocity as a function of period, given the number of plane horizontal layers in the structure n, and n sets of the layer parameters appropriate to the structure (compressional-wave velocity, shear-wave velocity, density, and layer thickness). Figure 13 shows the computed theoretical dispersion curves for the three models given in Table 3.

For the array taken as a whole, both the U.W.3 and USGS3 models fit the observed phase velocity curves fairly well (See Figure 14). The third model, T.I. 1, gives a much poorer fit with considerably higher phase velocities than were observed. The fit of the group velocity curves for all three models is poor. This may be due to the manner in which the experimental group velocity data were obtained (See Appendix I).

Model U.W.3 fits the observed data for the eastern sector in the period range from 60 to 30 seconds (See Figure 15). Below this period range, the observed phase velocities are slightly higher than those predicted by the model, suggesting that the mean shear velocity for the upper layers of the model should be increased. Model USGS3 gives a poor fit for the eastern sector.

For the western sector, USGS3 agrees with the observed data in the period range from 60 to 40 seconds (Figure 16) but again the observed phase velocities are higher at the

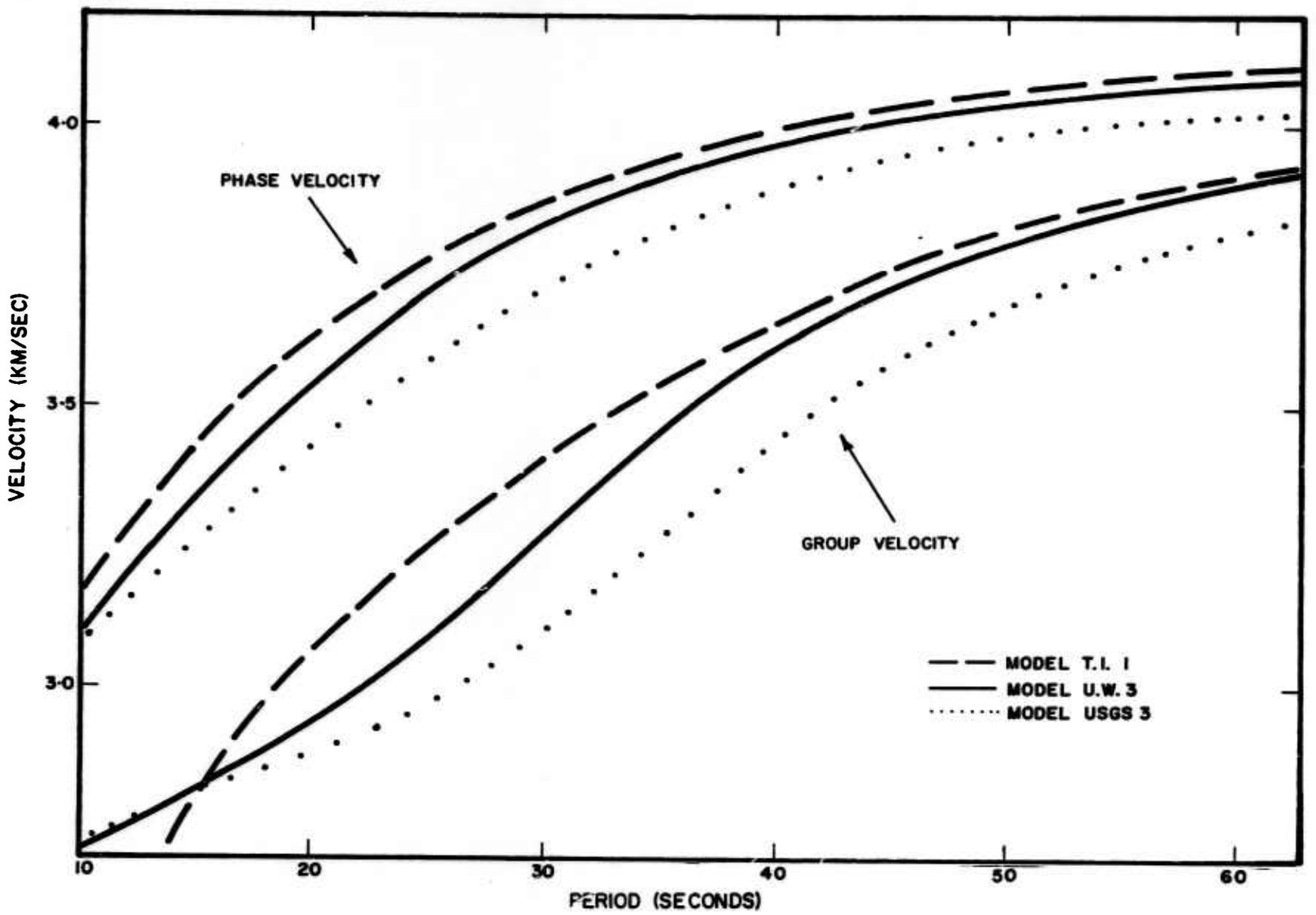

Figure 13. Theoretical Dispersion Curves for Fundamental Rayleigh Waves for the Three Models Given in the Text

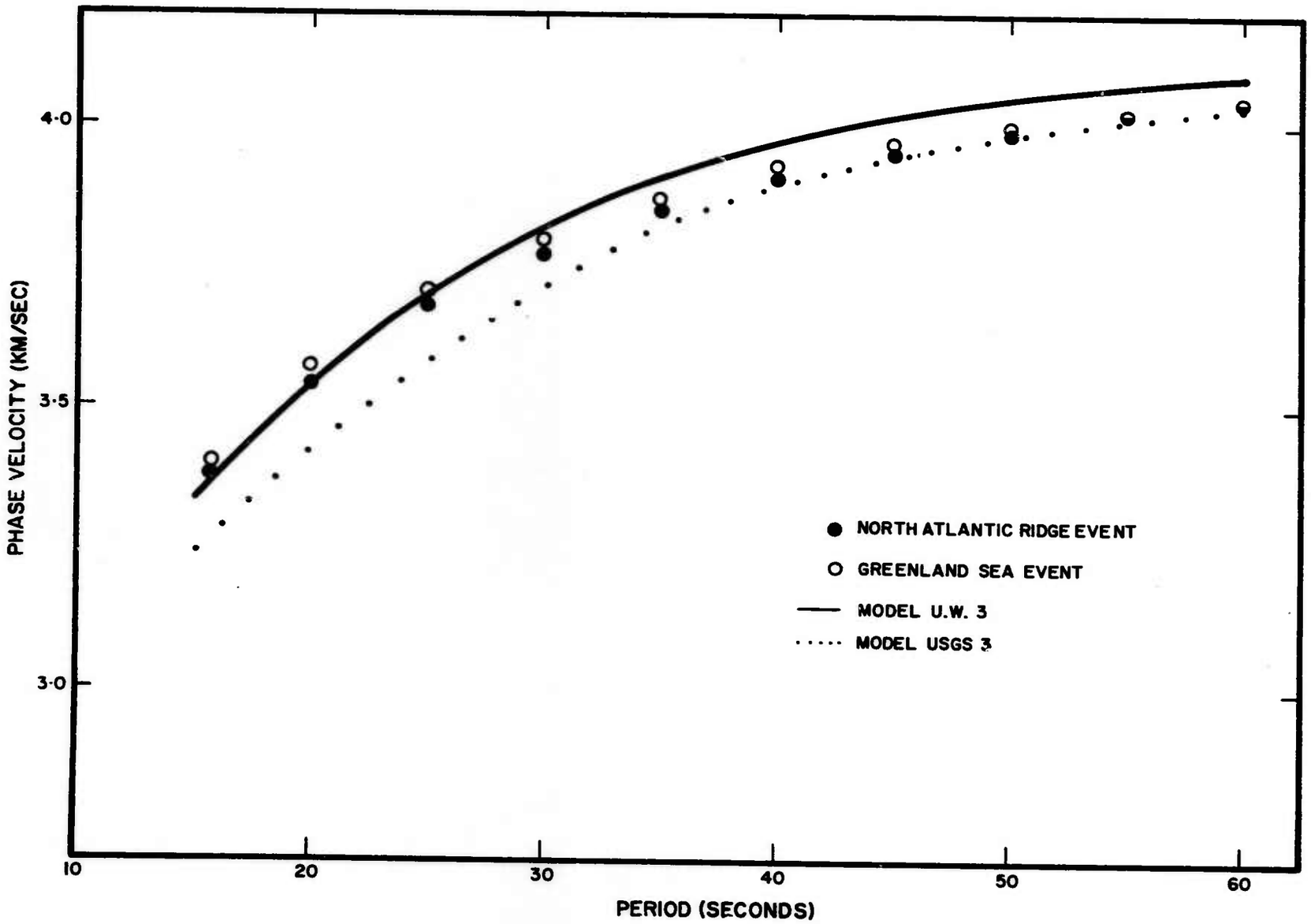

Figure 14. Observed Rayleigh Wave Dispersion for the Whole Array Compared to Theoretical Dispersion Curves Computed from Models U.W.3 and USGS3

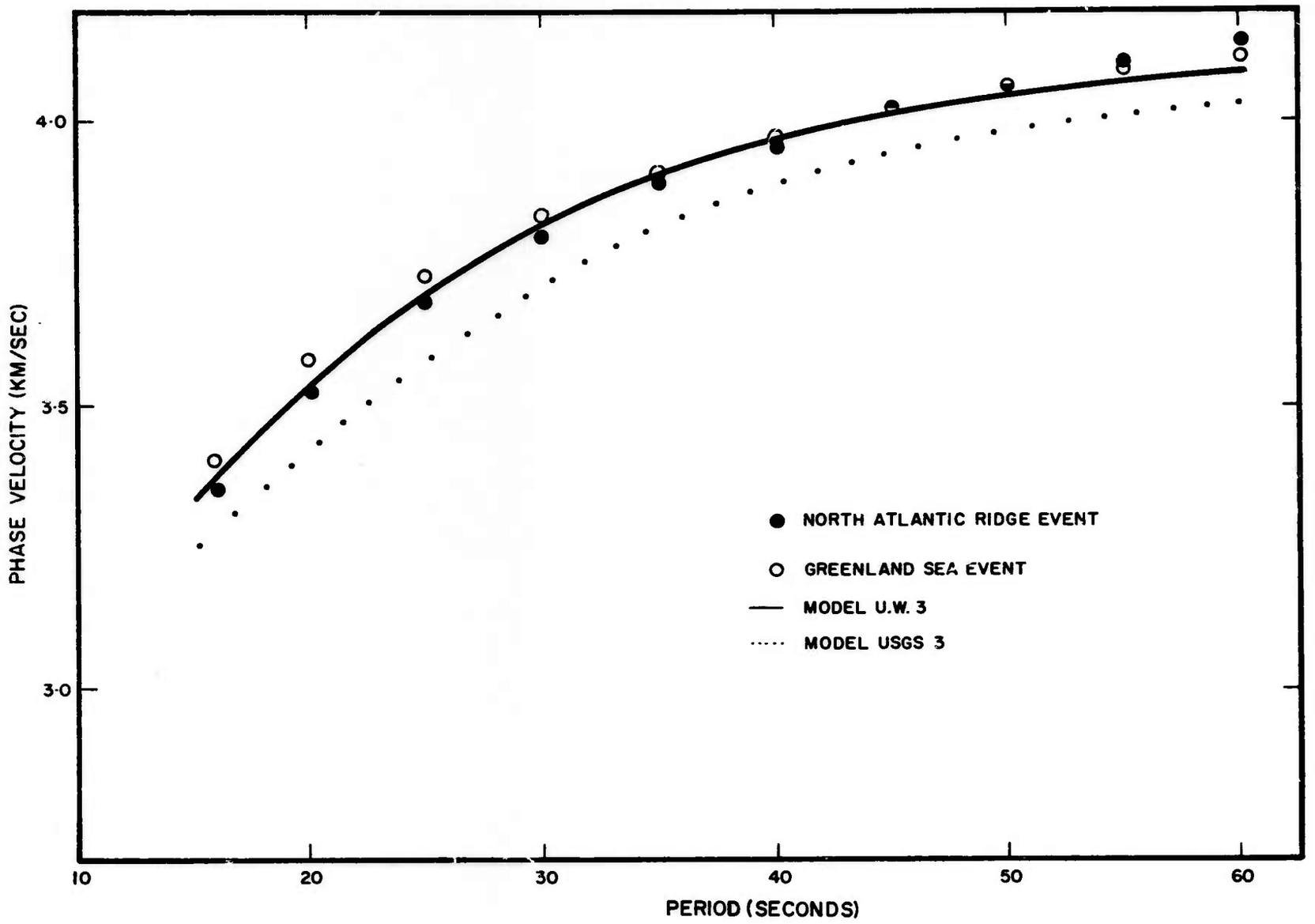

Figure 15. Observed Rayleigh Wave Dispersion for the Eastern Sector Compared to Theoretical Dispersion Curves Computed from Models U.W.3 and USGS3

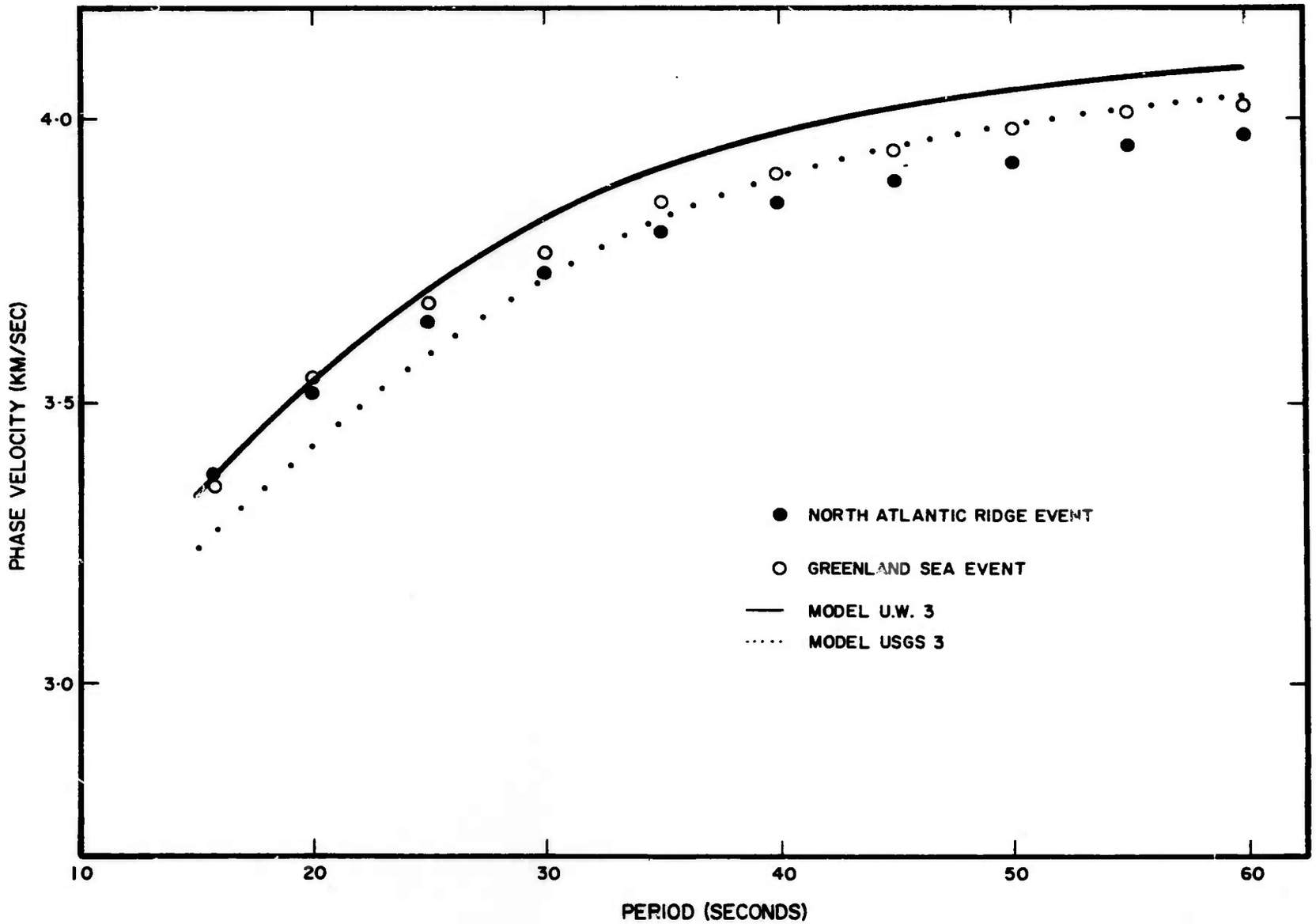

Figure 16. Observed Rayleigh Wave Dispersion for the Western Sector Compared to Theoretical Dispersion Curves Computed from Models U.W.3 and USGS3

shorter periods. Model U.W.3 gives consistently higher phase velocities in the range 60 to 20 seconds, but crosses the theoretical dispersion curve at a period of 19 seconds.

This comparison of observed and theoretical dispersion curves indicates that a model based on the refraction data published by Meyer, et al., (1961) best approximates the structure under the eastern sector of the array, whereas a model taken from the results of a more recent study by the U.S. Geological Survey (Borcherdt and Roller 1967) best fits the western sector. This conclusion implies that although the phase velocities are higher under the eastern sector, the crust under the eastern sector of the array can be thicker than that under the western sector because the total crustal thickness of U.W.3 is 54 km whereas that of the USGS3 model is only 49 km. Since the phase velocities from the western sector are lower than those to the east despite the westward thinning, average shear-wave velocities for the crust must decrease to the west. Again this is consistent with the refraction results.

Edivence from Long-Period Body Wave Spectral Ratios

Phinney (1964) has demonstrated that an estimate of crustal structure beneath a recording site may be obtained from the ratio of the power spectrum of the vertical component to the power spectrum of the radial component of the initial onset of an event recorded by a single three-component long-period seismograph. In an attempt to determine the manner in which the crustal transfer function varies across LASA, we obtained spectral ratios of the initial onsets from two teleseismic events (see Figure 17). The epicenter data for these events are given in Table 5.

For the event on 23 December 1966 the back-azimuth was considered to be sufficiently close to 270 degrees that the E-W component seismogram was taken as the radial component at each subarray. For the event of 15 February 1967, the two observed horizontal components from each subarray were rotated to the back-azimuth (140.8 degrees) in order to obtain an equivalent radial component. The smoothed power

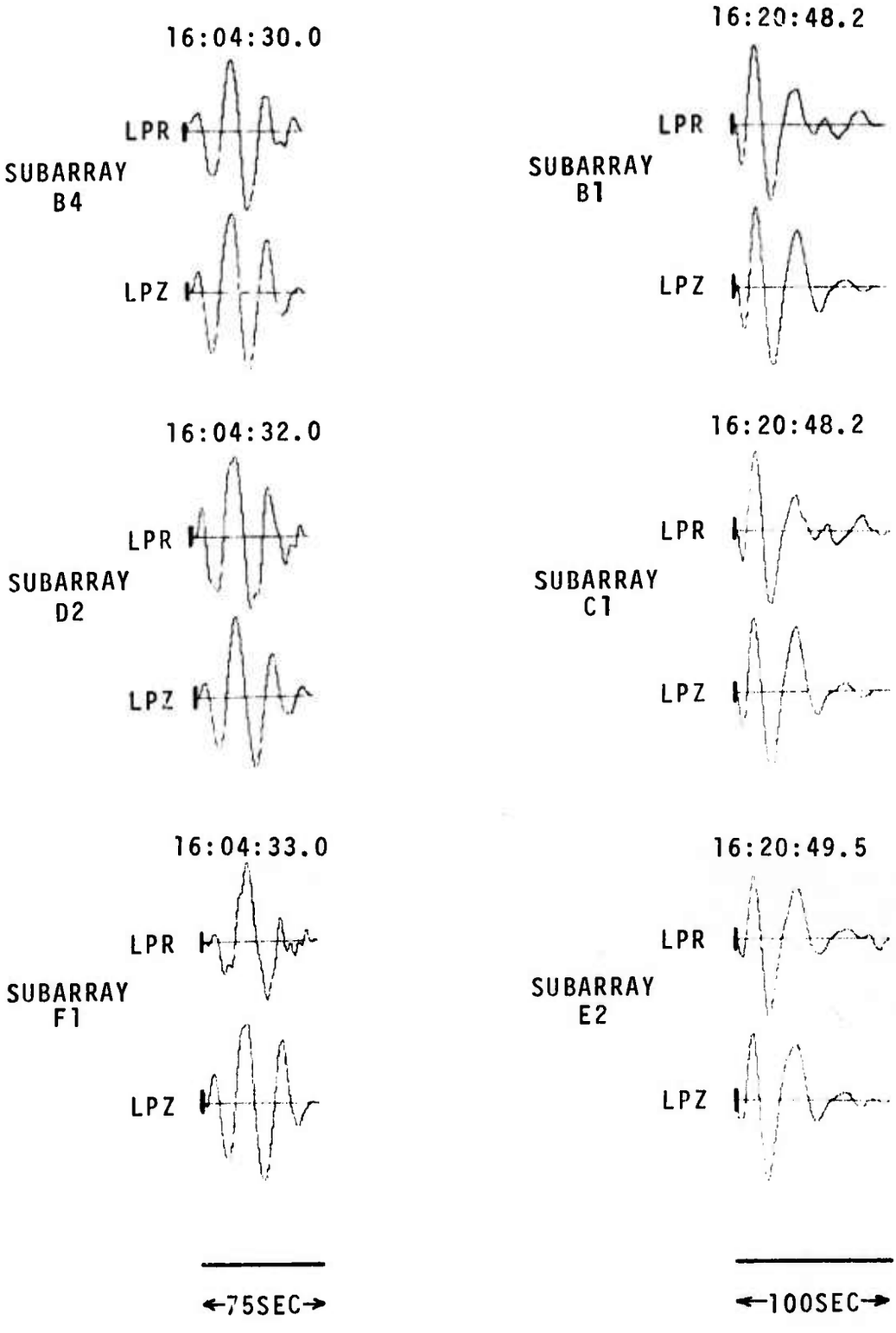

Figure 17. Typical Initial Onsets of the LP Seismograms Used in the Spectral Ratio Study

Table 5. Epicenter Data for Events used in Body Wave Spectral Ratio Study.

Date	Origin Time	Location	Depth (km)	Distance* (Degrees)	Azimuth* (Degrees)	Back* Azimuth (Degrees)	Magnitude (c.g.s)
23 Dec 66	15:50:20.4	New Guinea 7.1S 148.3E	43	105.7	43.6	276.4	6.4
15 Feb 67	16:11:11.8	Peru-Brazil 9.0S 71.3W	597	63.6	333.9	140.8	6.2

* Calculated from subarray AO.

spectrum of a 100-second window commencing with the initial P-wave onset (see Figure 17) for the radial and vertical components for both events were computed from the square of the numerical Fourier transform of the seismograms. The smoothing was performed using a Hanning routine developed by J. Claerbout (McCowan, 1968). The ratio of the vertical to horizontal smoothed spectra was then computed for each subarray. (The spectra were not corrected for instrument response since the amplitude response of horizontal and vertical component seismographs at LASA is matched to better than 17% at any given subarray).

Typical examples of the observed spectral ratios for the 23 December 1966 event are shown in Figure 18. The spectral ratios from subarrays A0, B1, B2, and B3 were similar. The remainder of the observed ratios for this event differed significantly in detail although their overall shape was similar.

Similar results for the 15 February 1967 event are shown in Figure 19. In this case, the spectral ratios from subarrays A0, B1, B2, and C1 closely resembled one another, as did those from B4 and C4. Again the remainder of the observed spectral ratios differed significantly in detail.

The spectral ratios at identical stations differed for the two events. This may be attributed in part to differences in crustal structure at the source as suggested by the fact that the spectral ratios for the deep-focus event (15 February 1967) are much smoother. Alternatively, since the results from both events are consistent in that for those subarrays separated by less than 12 km the observed spectral ratios are similar, the differences between the two sets of ratios may be due to the differences in azimuth of approach between the two events. Since the signal-to-noise ratio for both events is high, it is probable that the differences in spectral ratios at the various subarrays reflect the manner in which structure changes across LASA.

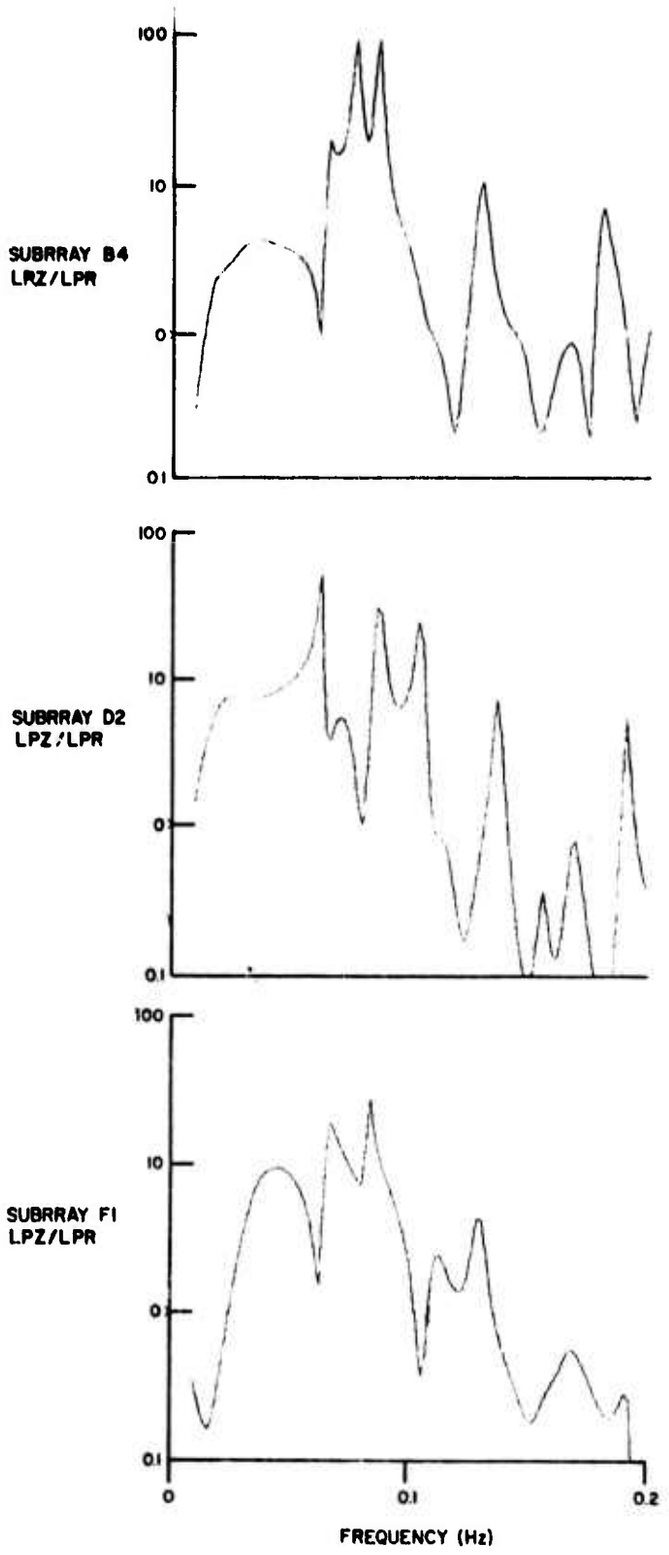

Figure 18. Spectral Ratios, LPZ/LPR, Formed from the Seismograms shown in Figure 17 for the 22 December 1966 Event

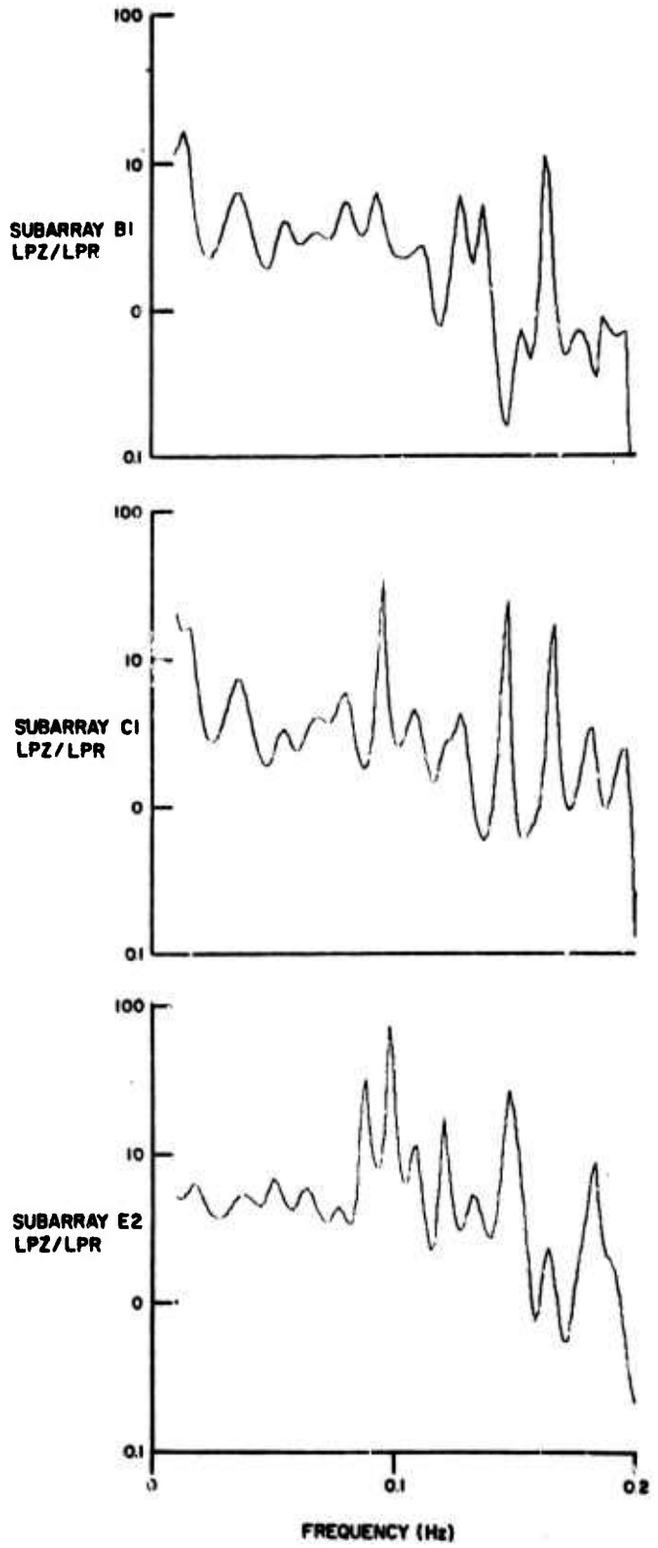

Figure 19. Spectral Ratios, LPZ/LPR, Formed from the Seismograms shown in Figure 17 for the 15 February 1967 Event

Theoretical spectral ratios were calculated from the models U.W.3 and USGS3 (given in Table 2) using the Thompson-Haskell matrix method (Haskell, 1953). The resulting curves are shown in Figure 20.

Comparison of the observed ratios with the calculated ones shows that neither model fits the observations exactly. However, the level of the observed curves from the eastern sector of the array is lower than that of the observed curves from the western sector by a factor of two, over the period range 50-15 seconds. The level of the theoretical curve computed from model U.W.3 is lower than the curve computed from the USGS3 model over the corresponding period range. This suggests that the model U.W.3 is a better approximation to the structure of the earth's crust than USGS3 in the eastern sector of the array, whereas USGS3 more closely approximates the structure in the western sector. Thus the spectral ratio data are consistent with the results from the Rayleigh wave dispersion observations discussed previously.

At present, all that may be further concluded from the observed spectral ratios is that although similarities in crustal structure exist at stations located close to the center of the array (e.g., A0, B1, B3), the overall structure of the crust varies systematically from east to west across LASA.

Short-Period P-wave Travel-time Anomalies

The mean travel-time anomaly from several teleseismic events within the same seismic source region (defined by a narrow range of distance and azimuth) was calculated for each subarray at LASA using data of Chiburis (1966). When these mean anomalies were plotted on a map of LASA (see Figures 21 through 25), it was found that for events having NE (Figures 21a and 22a) and SW (Figure 23a) back-azimuths from LASA, contours of equal residual define a region of relatively late arrivals with its axis trending NE-SW and passing somewhat to the north of subarray A0. For the set of events having NW back-azimuths from LASA (Figure 24a) the

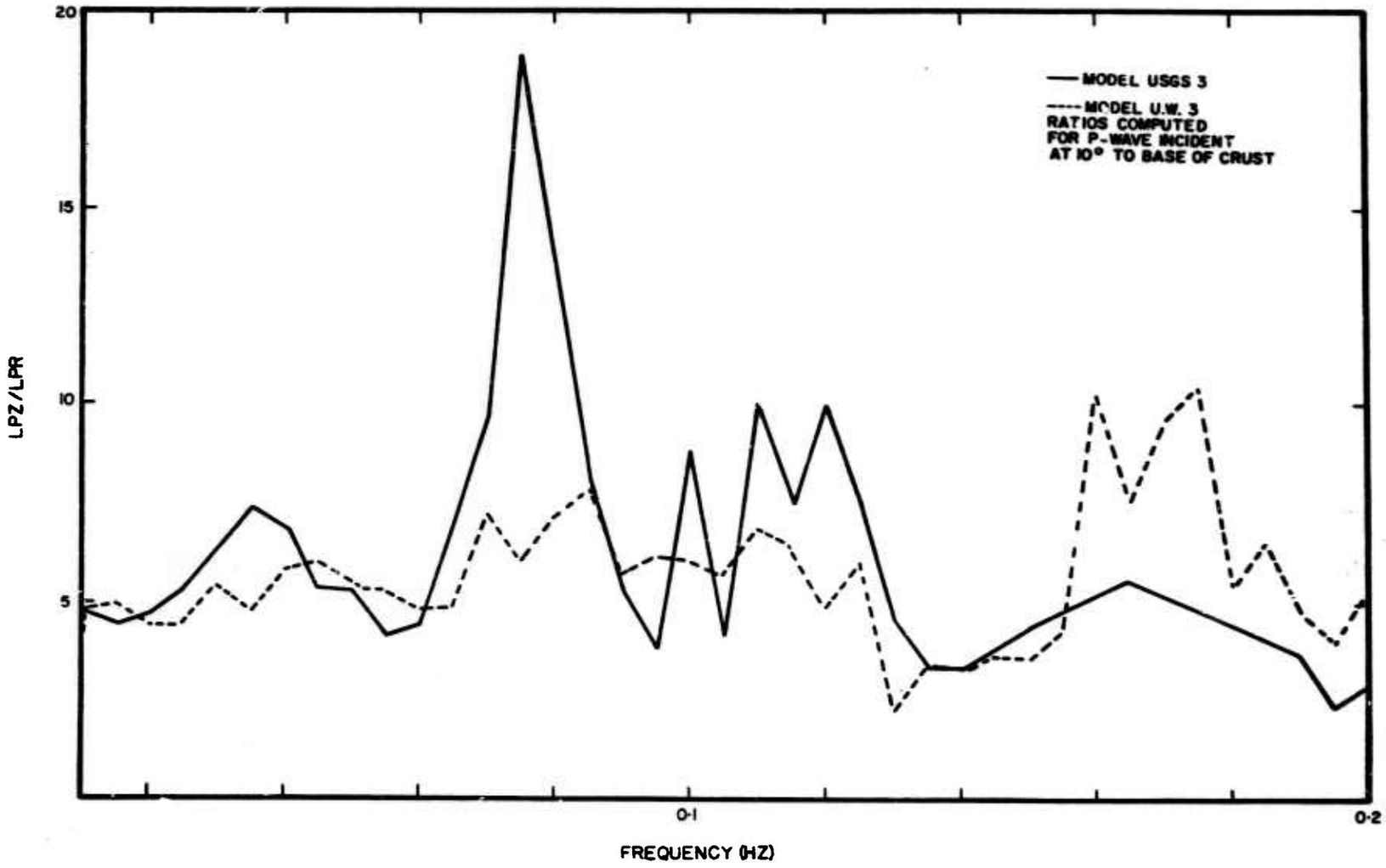

Figure 20. Theoretical Spectral Ratios Calculated from Models U.W.3 and USGS3, Assuming a Plane P-Wave Incident at the Base of the Crust

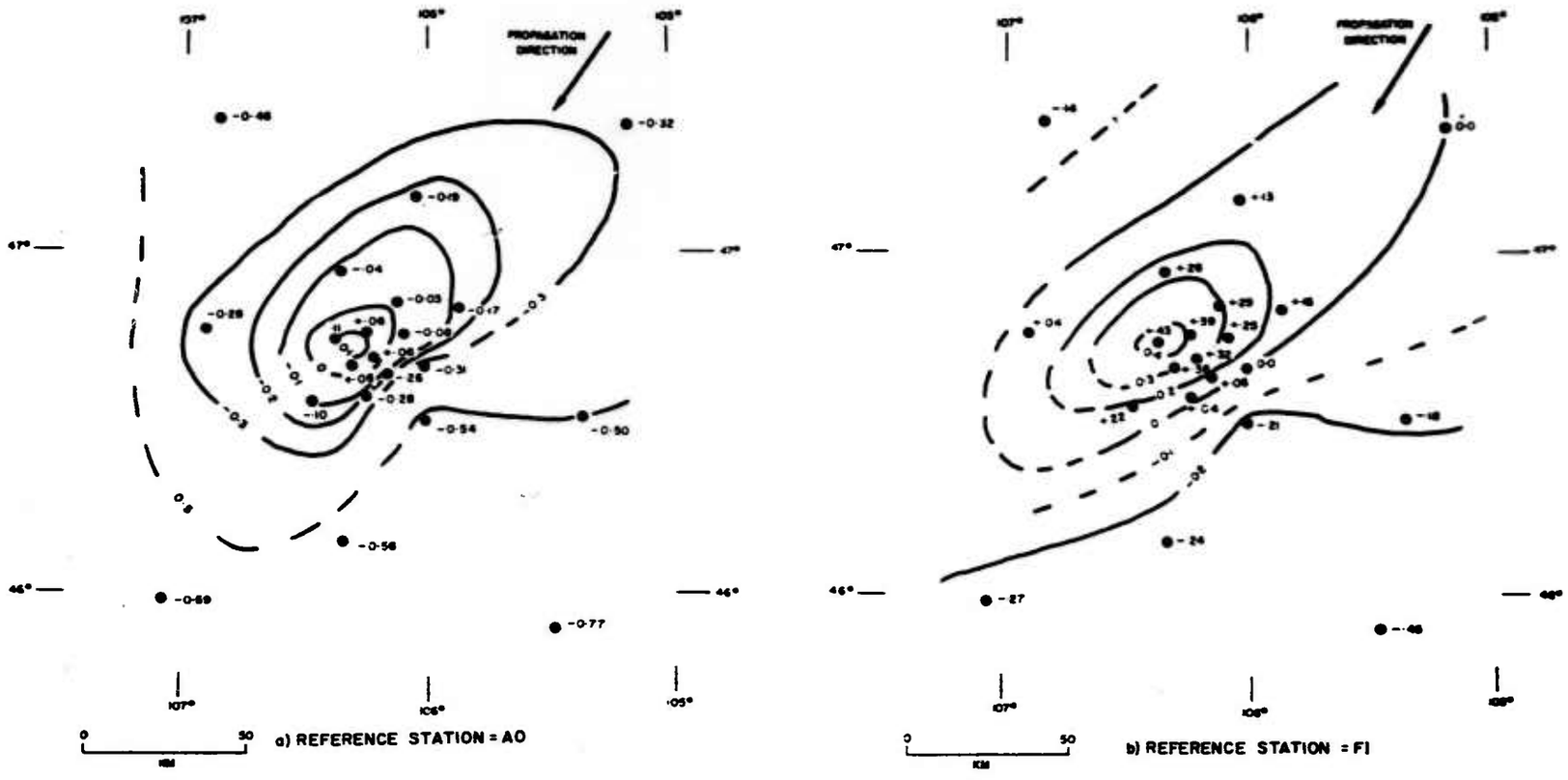

Figure 21. Mean Travel-time Anomalies Recorded at LASA from Several Events in the Western Turkey-Greece-Eastern Mediterranean Sea Region, Δ = 9140-9800 km, Back-Azimuth = 32-40°

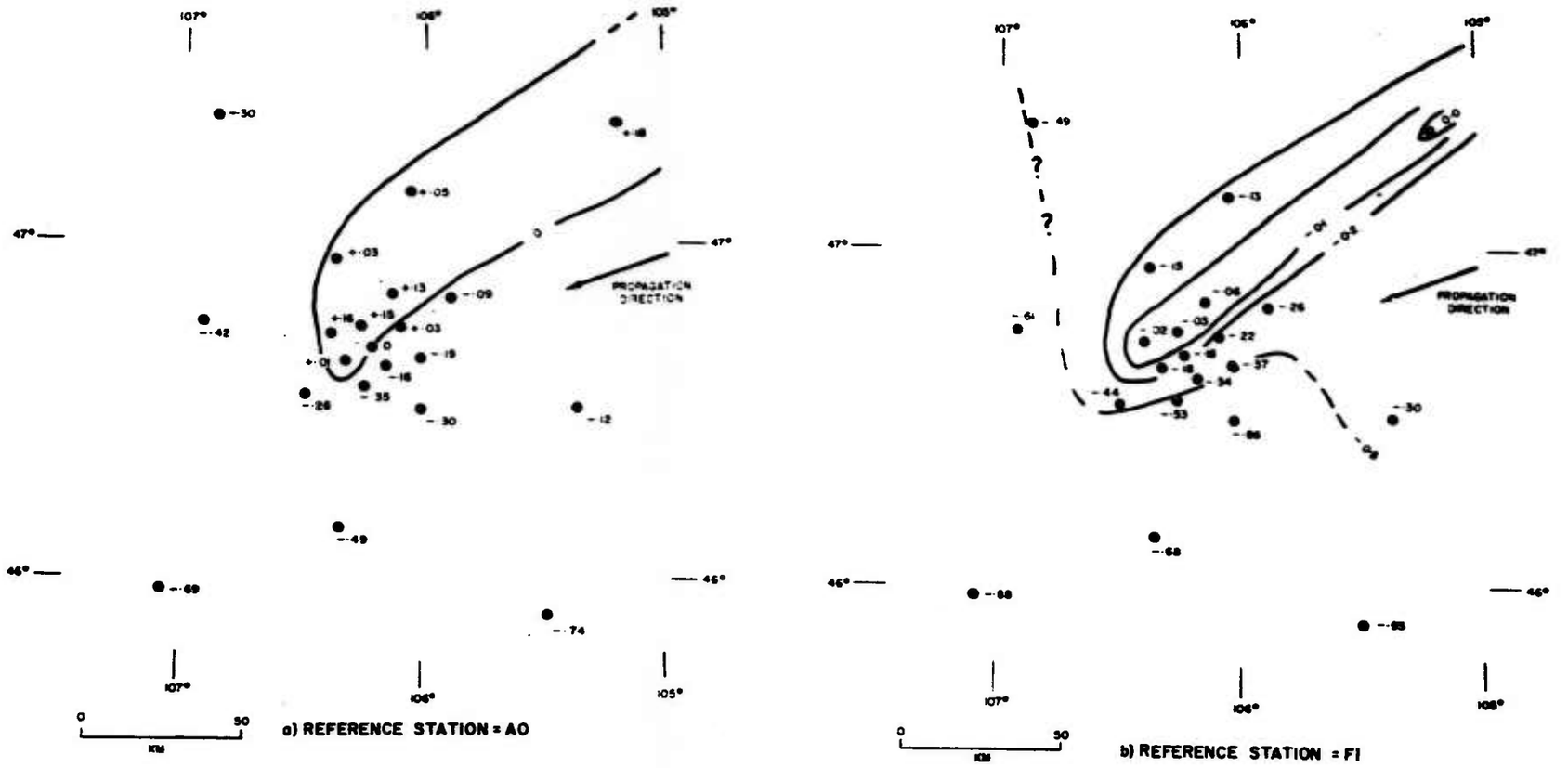

Figure 22. Mean Travel-time Anomalies Recorded at LASA from Two Events in the North Atlantic Ocean, Δ = 4800-5100 km, Back-Azimuth = 49-54°

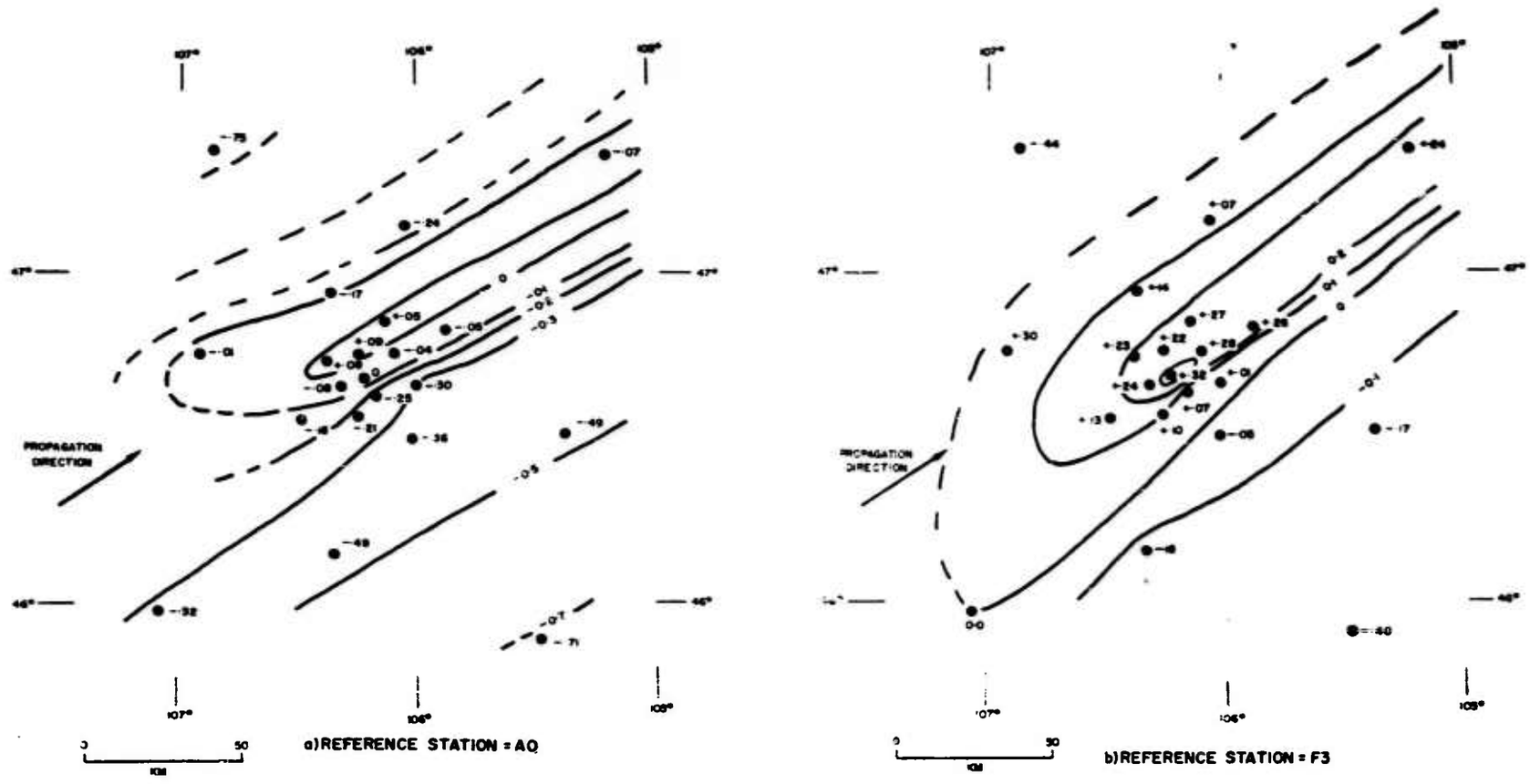

Figure 23. Mean Travel-time Anomalies Recorded at LASA from Several Events in the Samoa-Tonga Is. Region, Δ = 9600-10,400 km, Back-Azimuth = 234-244°

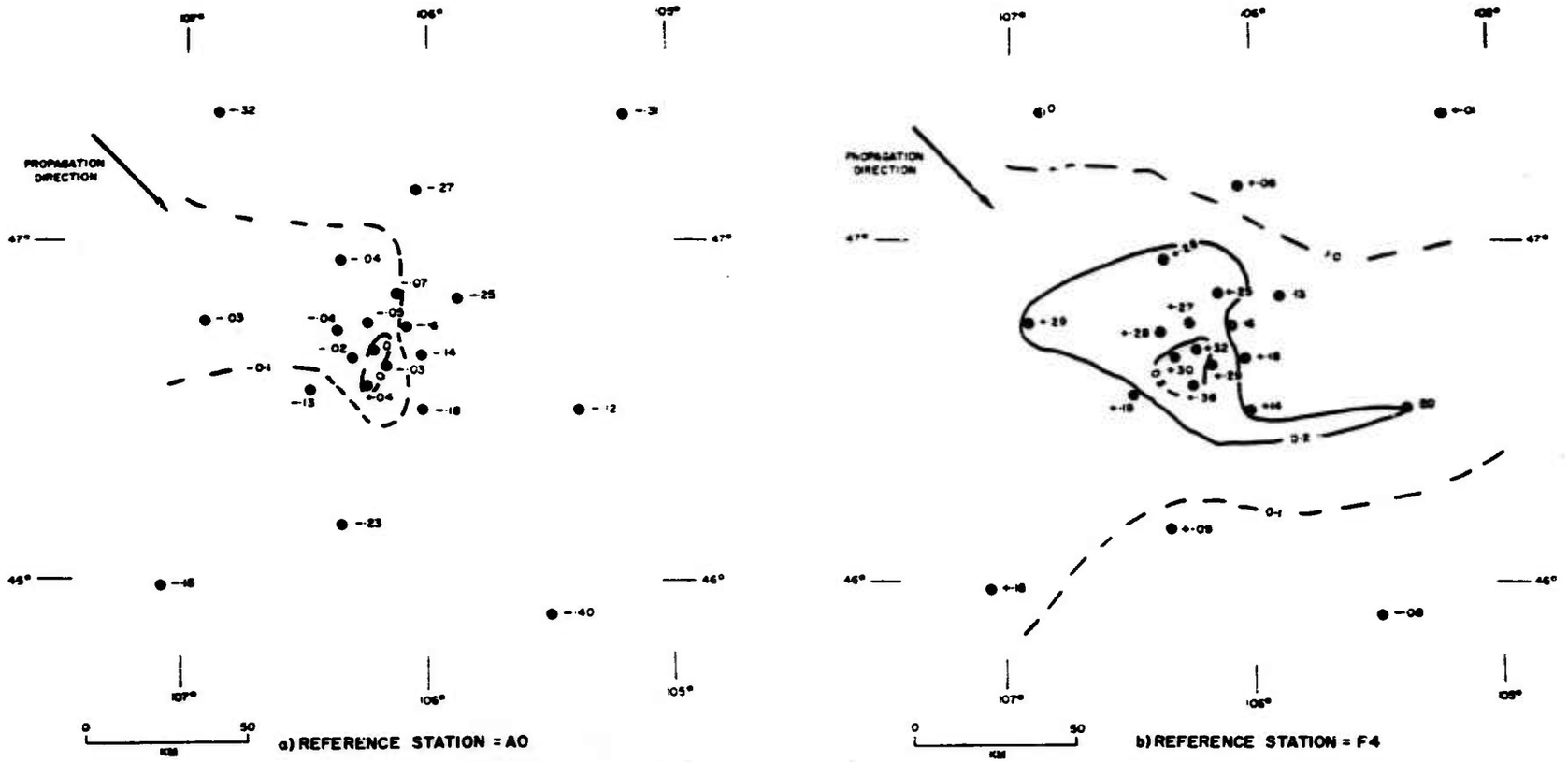

Figure 24. Mean Travel-time Anomalies Recorded at LASA from Several Events in the Kamchatka-Komamdorsky Region Δ = 5850-6600 km, Back Azimuth = 312-315°

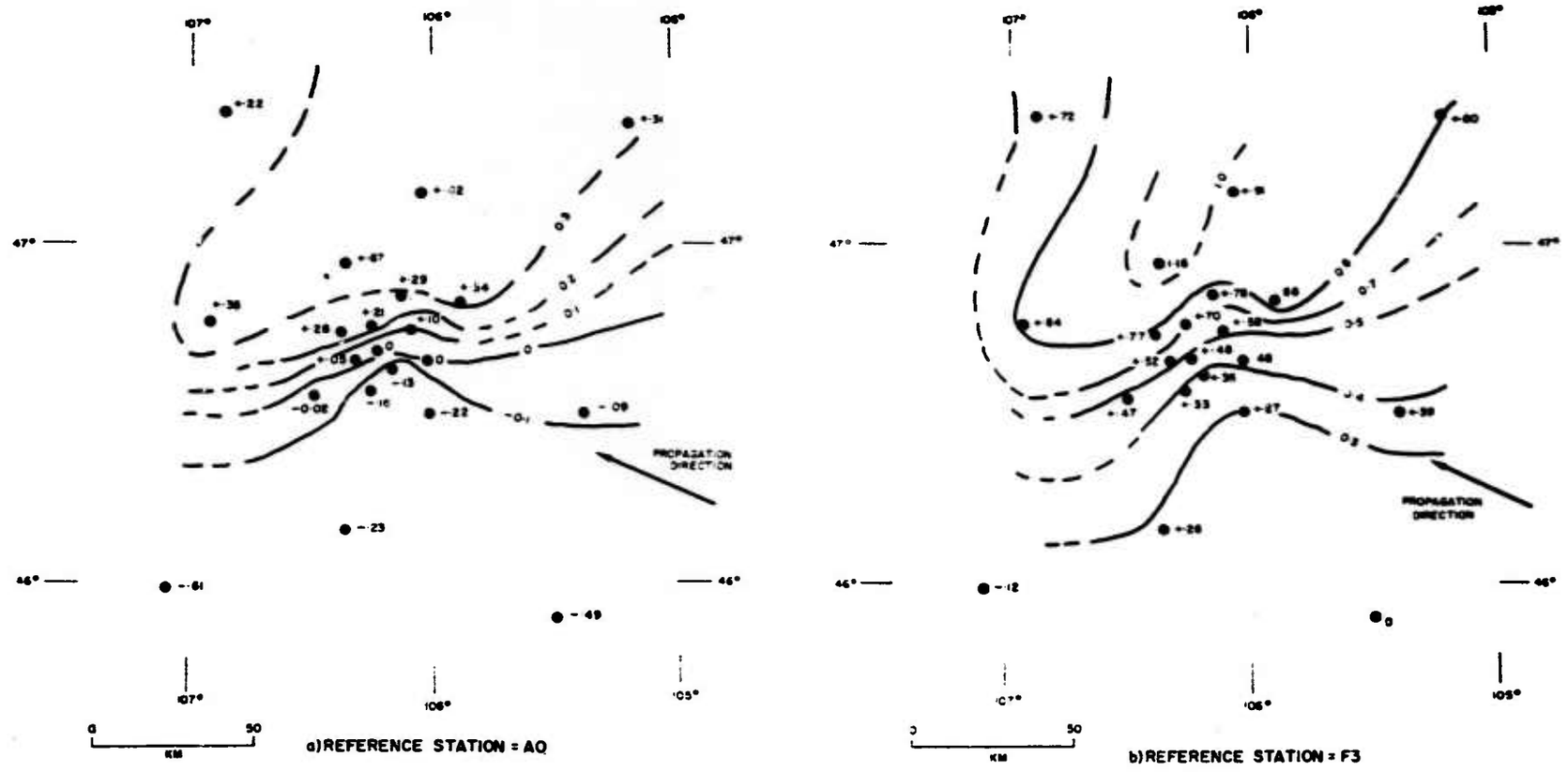

Figure 25. Mean Travel-time Anomalies Recorded at LASA from Several Events in the Northern W. Indies Region, Δ = 4850-5260 km, Back-Azimuth = 112-115°

pattern is less clear. Arrivals recorded at the center of the array were relatively late. For events from the SE (Figure 25a) the late arrivals define a region somewhat similar to that observed for events having NE and SW back azimuths from LASA.

When travel-time anomalies were calculated with reference to the subarray nearest the source (Figures 21b through 25b), the region of late arrivals is better defined for both sets of back-azimuths. However, the set of events from the NW (Figure 24b) still yields a closed area of relatively late arrivals at the center of the array. For the remaining back-azimuths, the shape and trend of the region defined by the late arrivals corresponds closely to that found by Sheppard (1967). This NE-SW trend also has an important bearing on the distribution of short-period P-wave amplitudes recorded at LASA, which are discussed in the next section.

Short-Period P-wave Amplitude Distributions

In a recent report, Klappenberger (1967) has shown that significant positive correlation exists between the distribution of short-period P-wave amplitudes recorded at the center of a given subarray at LASA, for seismic events having similar foci. We computed the mean of the (zero-to-peak) amplitude, expressed as mμ of equivalent vertical ground displacement at one cps, from the 21 sensors of each subarray for two of the events analyzed by Klappenberger (See Table 6 for epicenter data) having identical epicenters. These means are plotted in Figures 26 and 27. The contouring of points of equal amplitude response, even though somewhat subjective, shows a conspicuous NW-SE trend in both plots, with the suggestion in Figure 26 of a secondary trend in NE-SW direction near the center of the array. In addition, amplitudes for five other events with somewhat different epicenters (See Table 6), but from a common seismic source region having a mean back-azimuth NW from LASA are shown in Figures 28 through 32. Again the results show a strong NW-SE trend with the suggestion of a lesser NE-SW component.

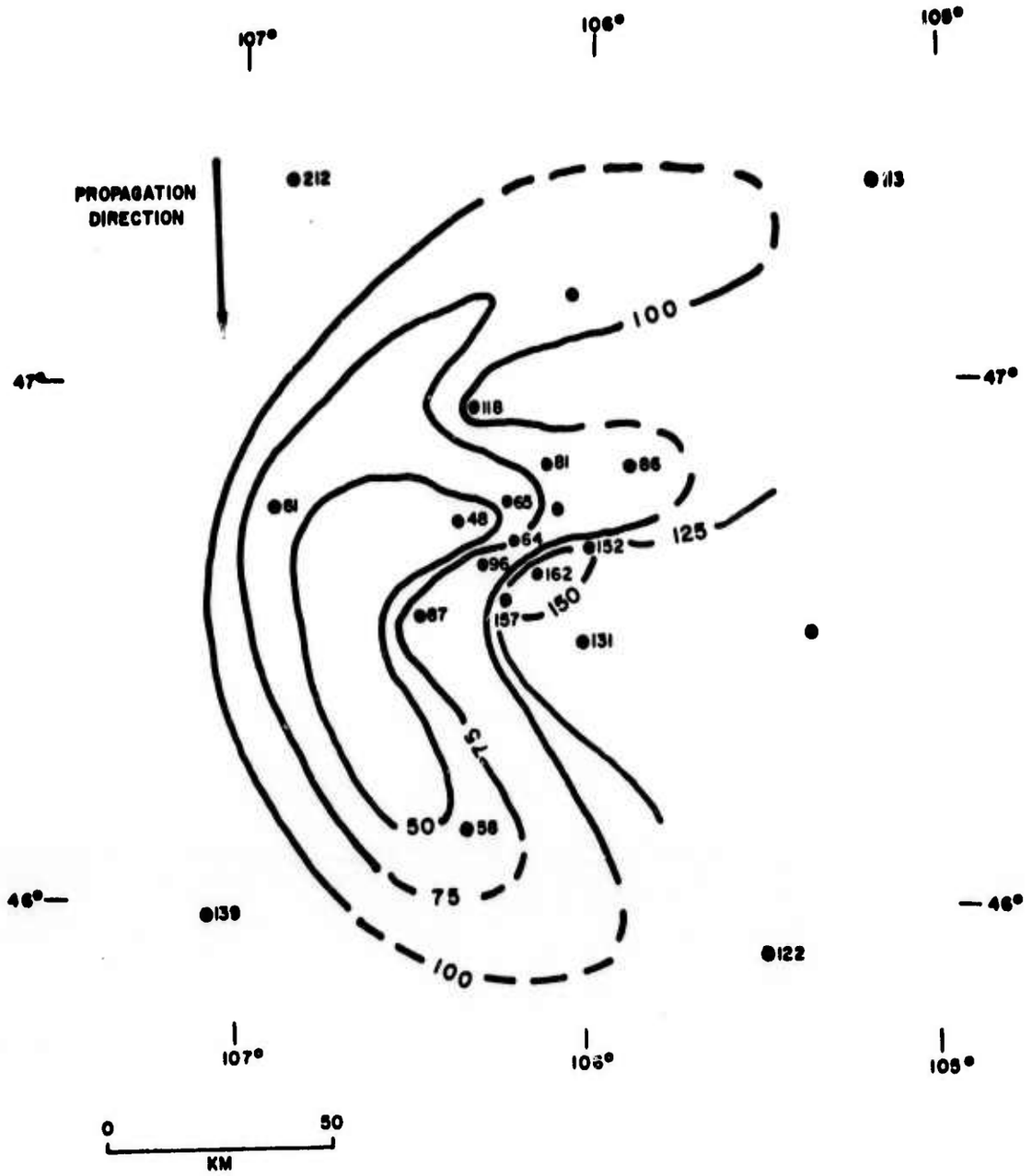

Figure 26. Contour Map Showing (zero-to-peak) P-wave Amplitude Recorded at LASA for the Event 21 November 1965 at 04:57:57.9

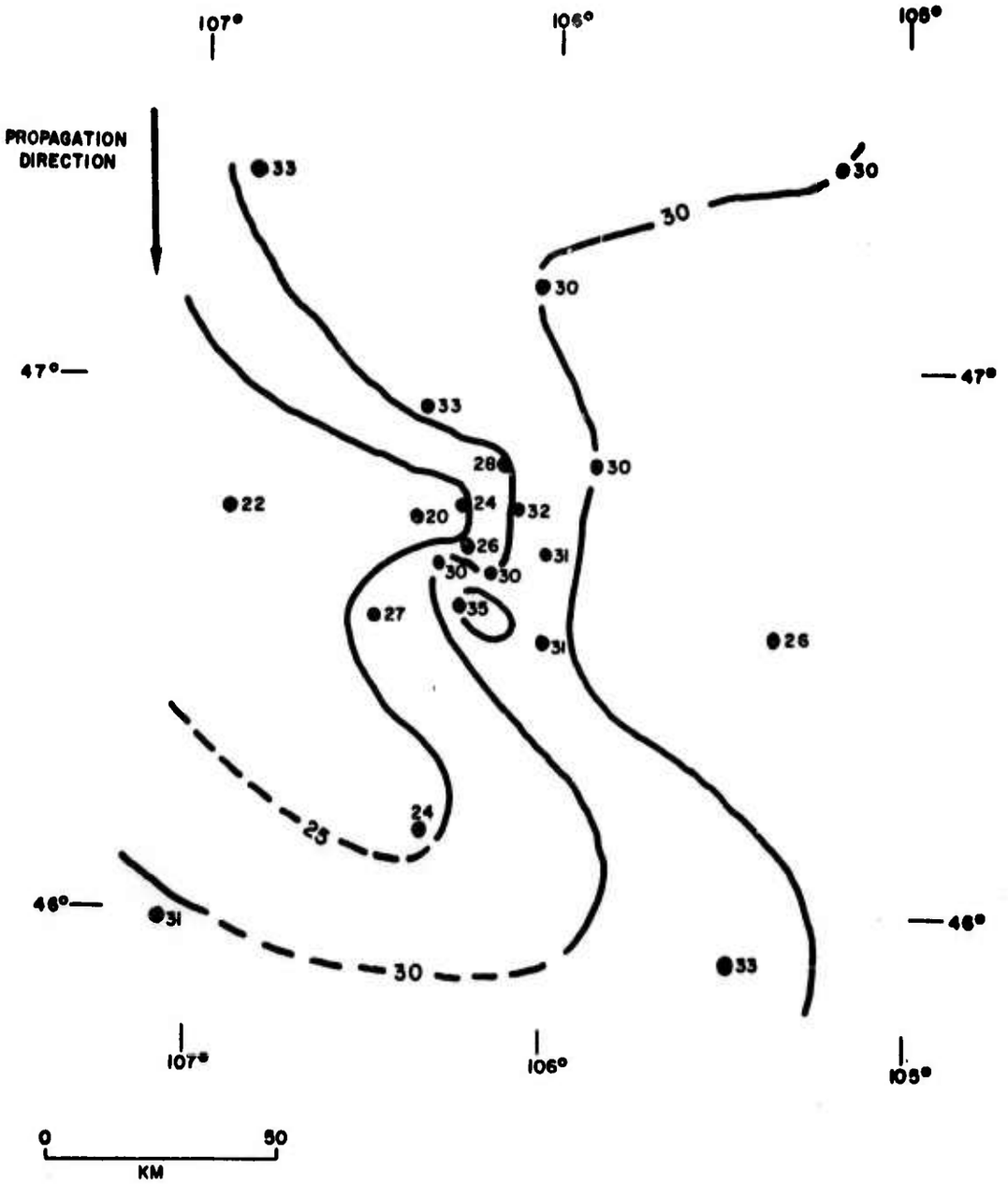

Figure 27. Contour Map Showing (zero-to-peak) P-wave Amplitude Recorded at LASA for the Event 13 February 1966 at 04:57:57.9

Table 6. Epicenter Data for Events Used in Amplitude Distribution Study

Date	Origin Time	Location		Depth (km)	Distance (Degrees)	Azimuth (Degrees)	Back Azimuth (Degrees)	Magnitude (c.g.s.)
10 Nov 65	01:47:28.0	Peru-Brazil	17.8S 69.6W	140	72.1	334.5	143.3	4.3
20 Nov 65	03:47:52.4	Tonga Is.	15.4S 174.5W	12	86.9	39.8	243.8	5.2
21 Nov 65#	04:57:57.9	Kazakh	49.8N 78.1E	0	83.8	3.0	357.2	-
21 Nov 65	06:10:56.0	Kurile Is.	48.4N 154.7E	33	62.1	50.3	311.9	4.7
25 Nov 65	03:35:11.7	Nr.Kamchatka	55.2N 163.0E	33	53.9	58.4	314.8	5.0
9 Dec 65	13:12:55.5	Fiji Is.	18.0S 178.2W	650	91.0	40.9	245.1	5.6
11 Dec 65	12:16:59.9	Kurile Is.	50.5N 155.3E	110	60.4	51.5	313.4	4.9
12 Dec 65	00:48:01.7	Andreanof	51.5N 178.9W	50	46.0	65.9	304.0	5.0
13 Feb 66#	04:57:57.7	Kazakh	49.8N 78.1E	0	83.8	3.0	357.2	-
28 Apr 66	10:24:39.6	Kamchatka	55.0N 162.0E	33	54.5	57.7	315.0	5.0

Explosion studied by Klappenberger (1967).

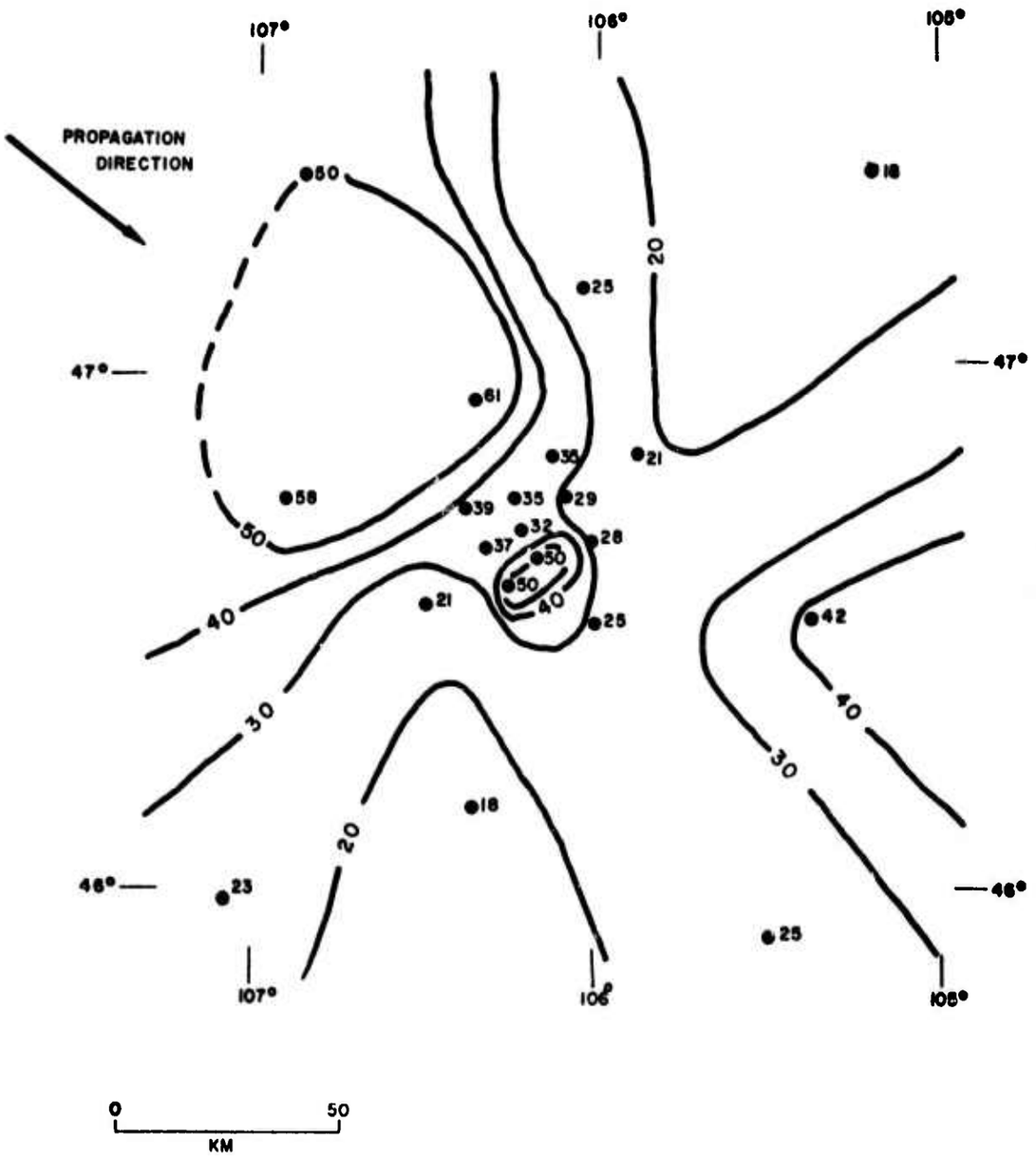

Figure 28. Contour Map Showing (zero-to-peak) P-wave Amplitude Recorded at LASA for the Event 21 November 1965 at 06:10:56.0

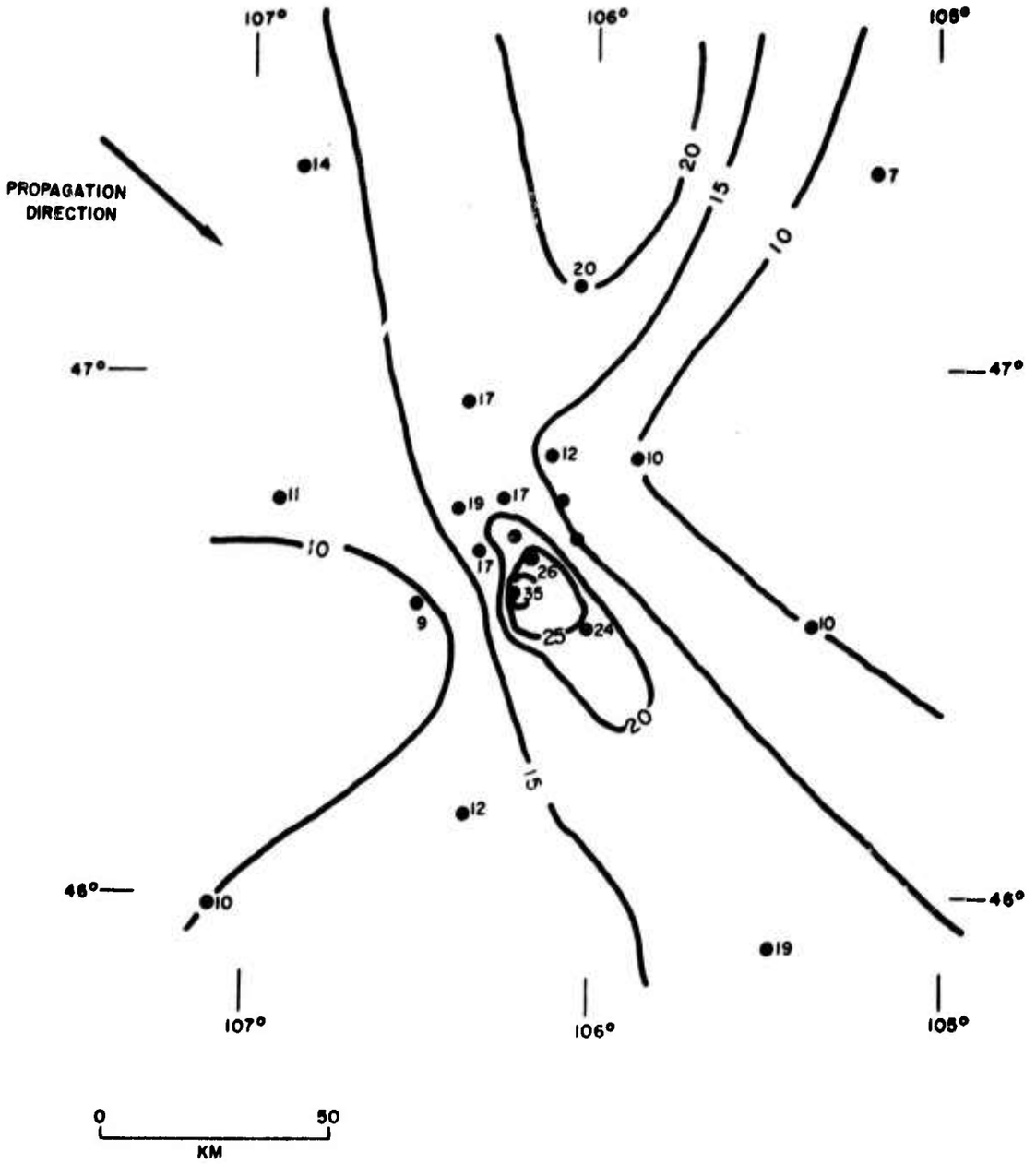

Figure 29. Contour Map Showing (zero-to-peak) P-wave Amplitude Recorded at LASA for the Event 25 November 1965 at 03:35:11.7

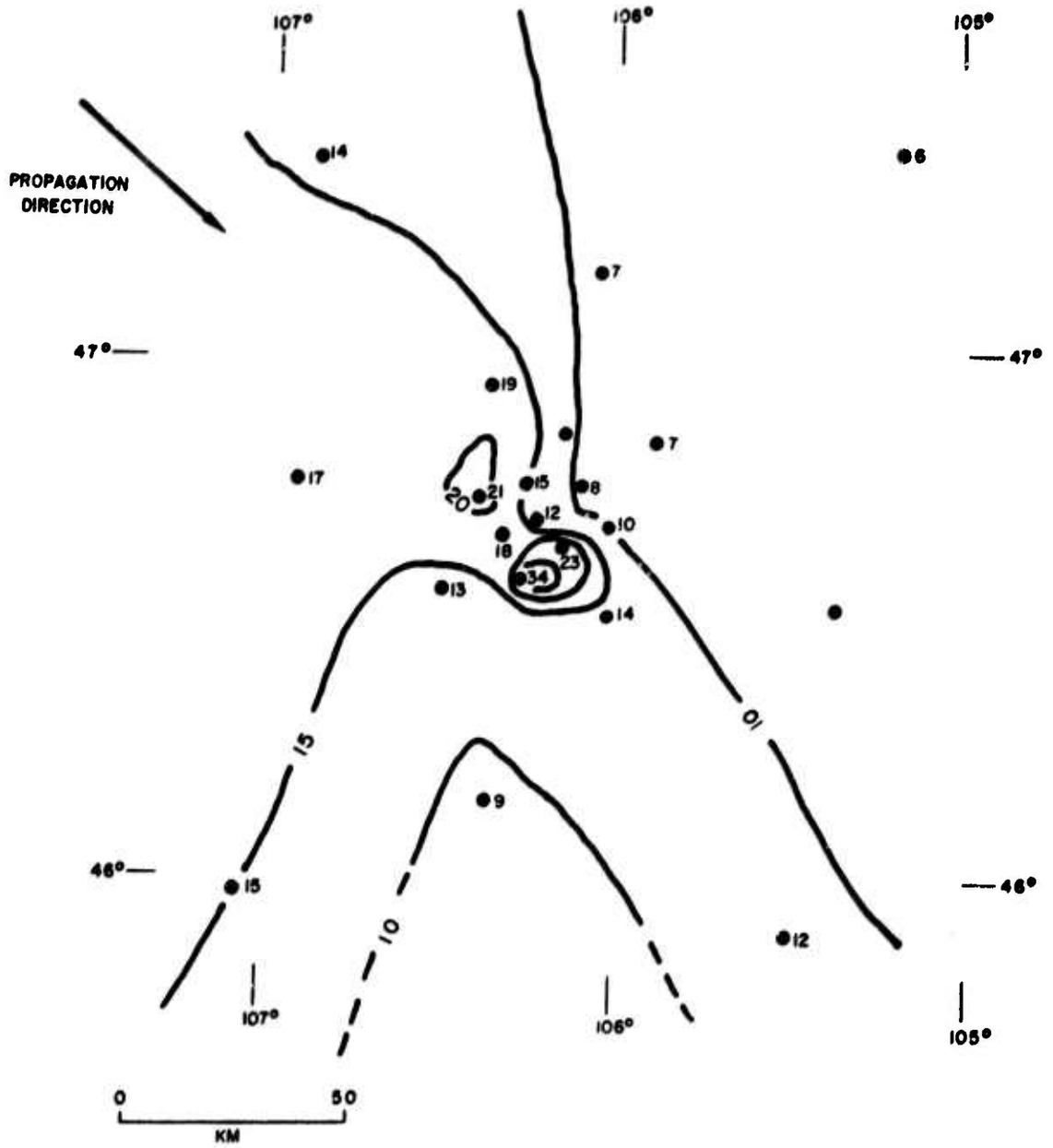

Figure 30. Contour Map Showing (zero-to-peak) P-wave Amplitude Recorded at LASA for the Event 11 December 1965 at 12:16:59.9

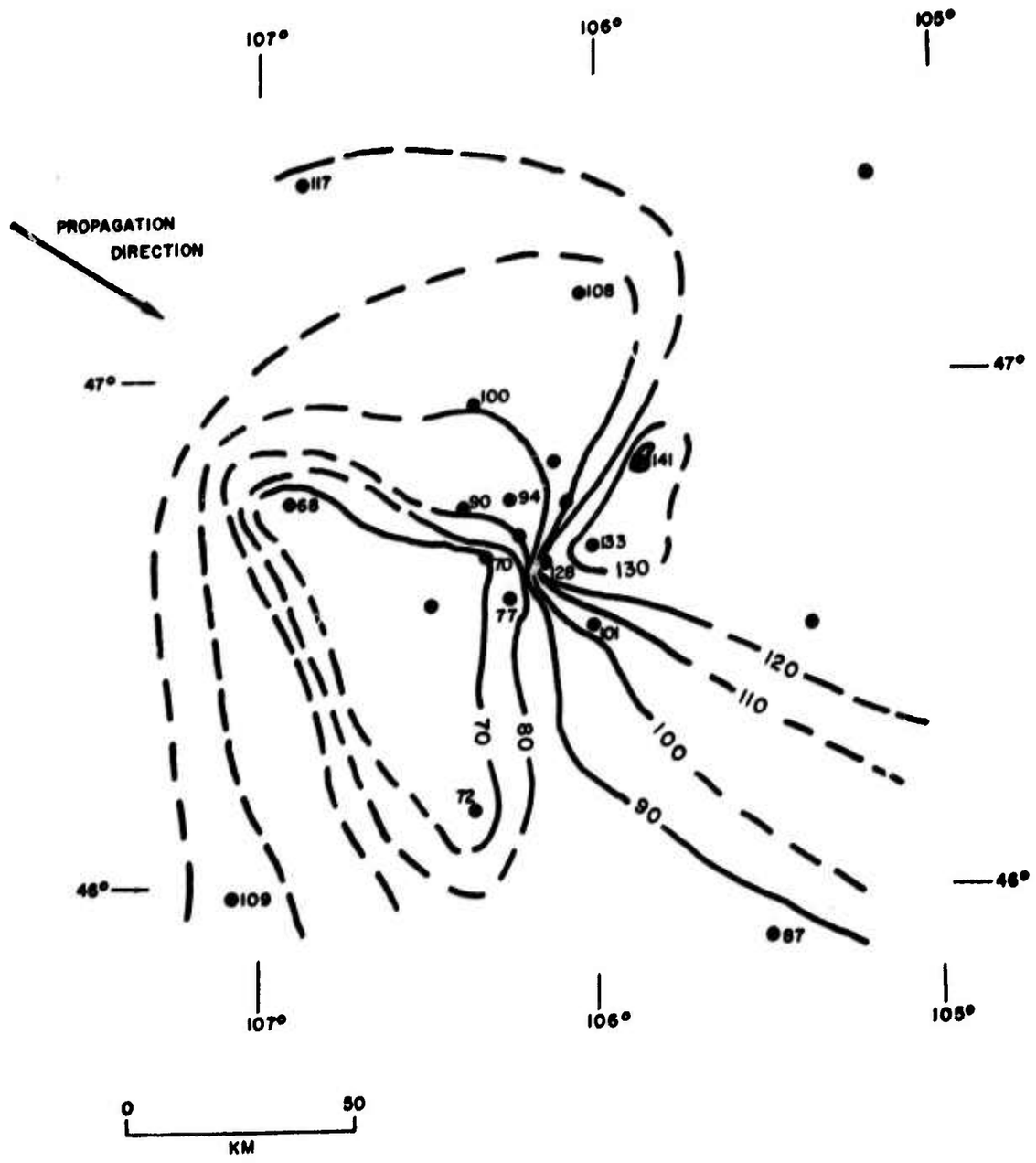

Figure 31. Contour Map Showing (zero-to-peak) P-wave Amplitude Recorded at LASA for the Event 12 December 1965 at 00:24:39.6

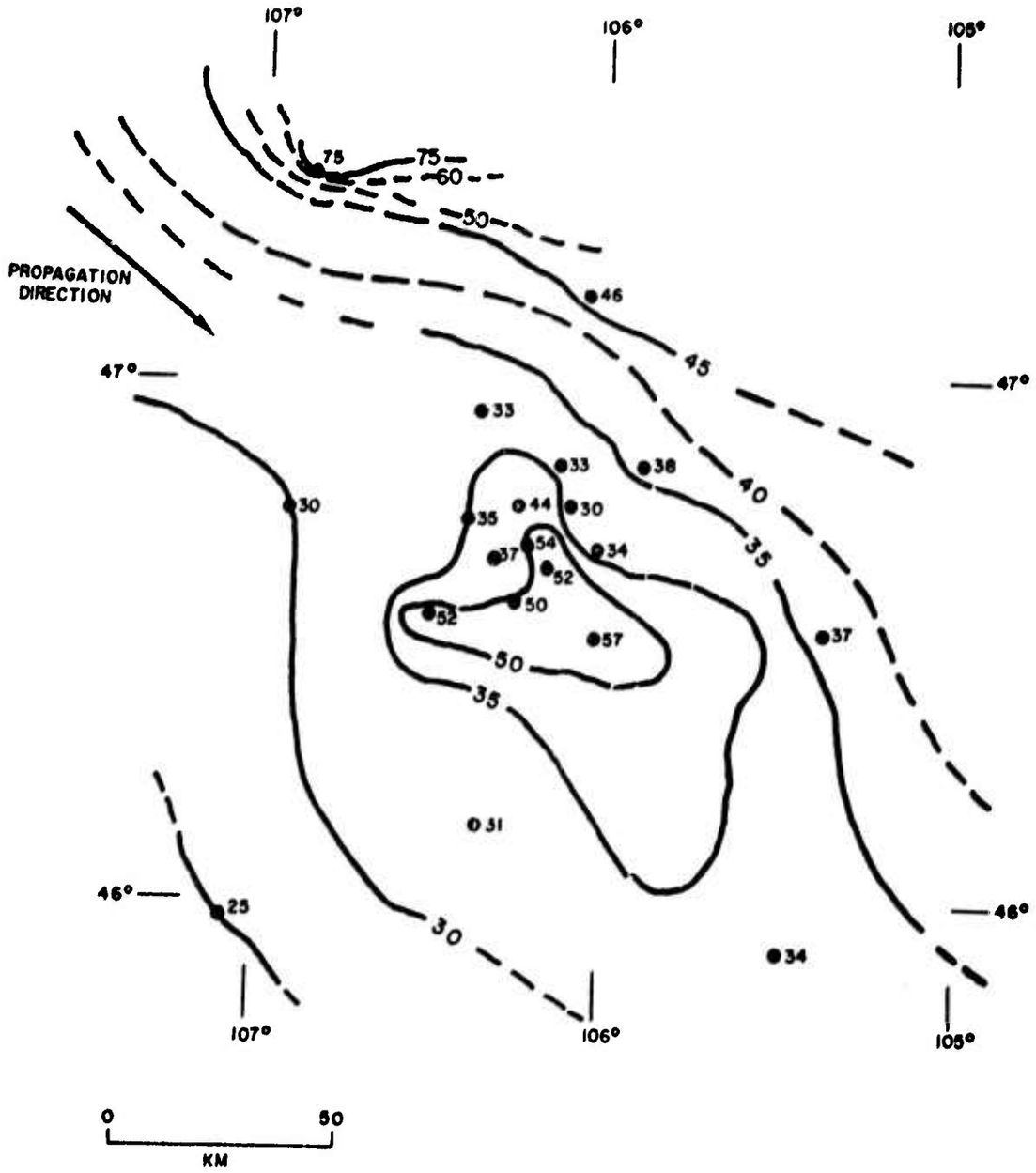

Figure 32. Contour Map Showing (zero-to-peak) P-wave Amplitude Recorded at LASA for the Event 28 February 1966 at 10:24:39.6

To further determine the azimuthal dependence of amplitude distributions, two events having approximately SW back-azimuths and a third having a SE back-azimuth (See Table 6) were plotted (Figures 33, 34, and 35 respectively). In the case of the two events with SW back-azimuths the strongest trend is NE-SW. The event from the SE shows no particular trend, the contours forming a closed low over the center of the array.

The events considered cover several different source regions and two types of seismic distrubances, namely earthquakes and explosions, and hence the consistent features discussed above cannot be attributed solely to source mechanism similarities or similar propagation paths. Rather, they should reflect differences in the earth's crustal structure under the array. Clearly there is a strong azimuthal dependence which suggests significant lateral variations. For events having NW to N back-azimuths from LASA the major trend is NW-SE, whereas for events having SW back-azimuths the NE-SW trend predominates. The latter trend is apparent in the areal distribution of travel-time anomalies discussed previously, whereas the NW-SE trend has no equivalent there, but is consistent with the major structural trend calculated from the Rayleigh wave dispersion data considered earlier.

With the exception of 12 December 1965 event (Figure 31) the plots for events having NW and SW back-azimuths from LASA show a region of relatively high amplitudes centered slightly to the south of A0. For the 12 December 1965 event there is a closed high somewhat to the NE of A0. For the two events approaching LASA from the north (Figures 26 and 27) the region of relatively high amplitudes at the center of the array is not so clearly defined. The event from the SE (see Figure 35) was the only event from which the smallest amplitudes were recorded at the center of the array.

Collectively these data indicate that there are two predominant structural trends bearing on the distribution of short period P-wave amplitudes recorded at LASA. The NW-SE trend corresponds to the major structural trend determined from Rayleigh wave dispersion across LASA and is the dominant

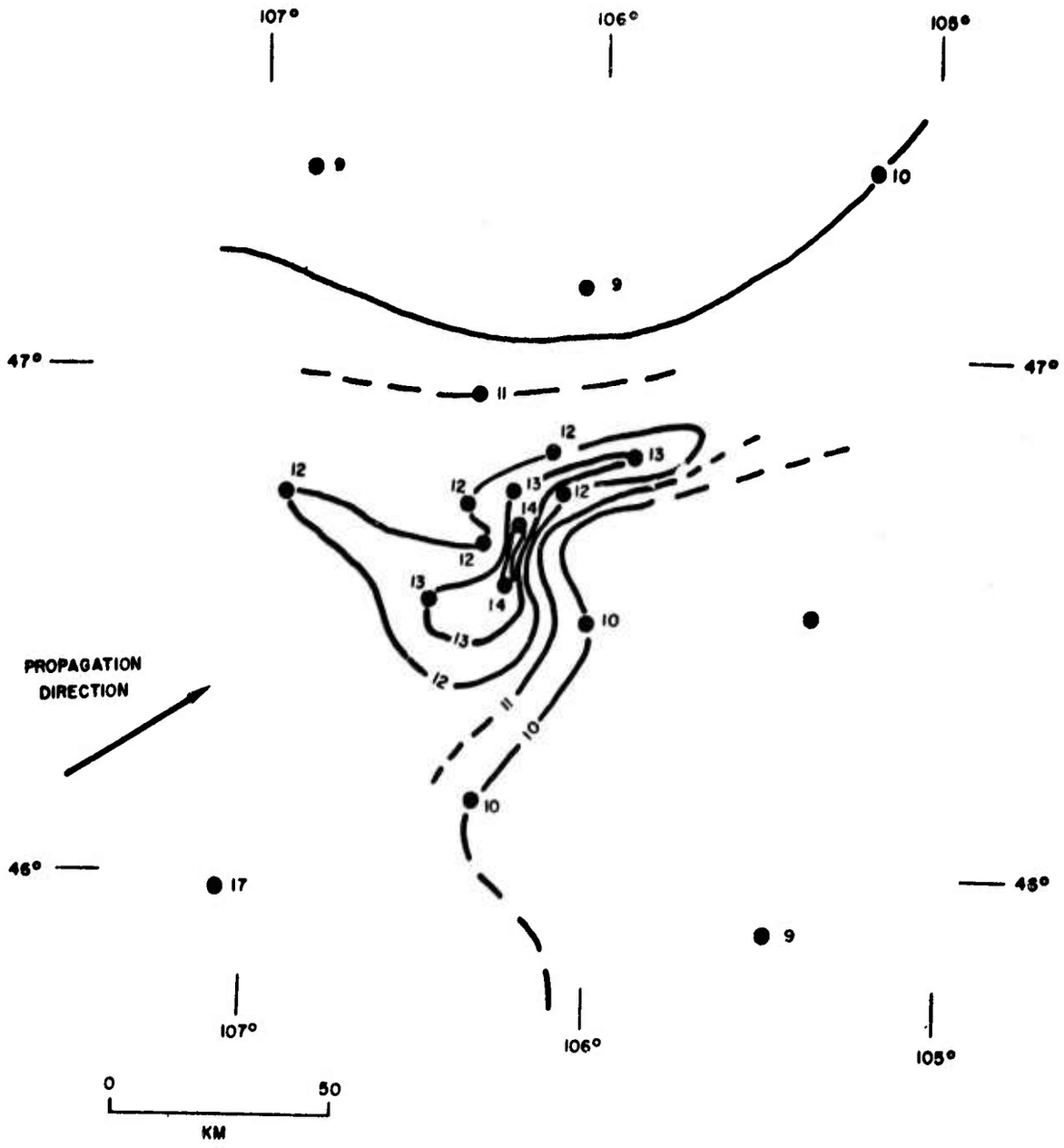

Figure 33. Contour Map Showing (zero-to-peak) P-wave Amplitude Recorded at LASA for the Event 20 November 1965 at 05:47:52.4

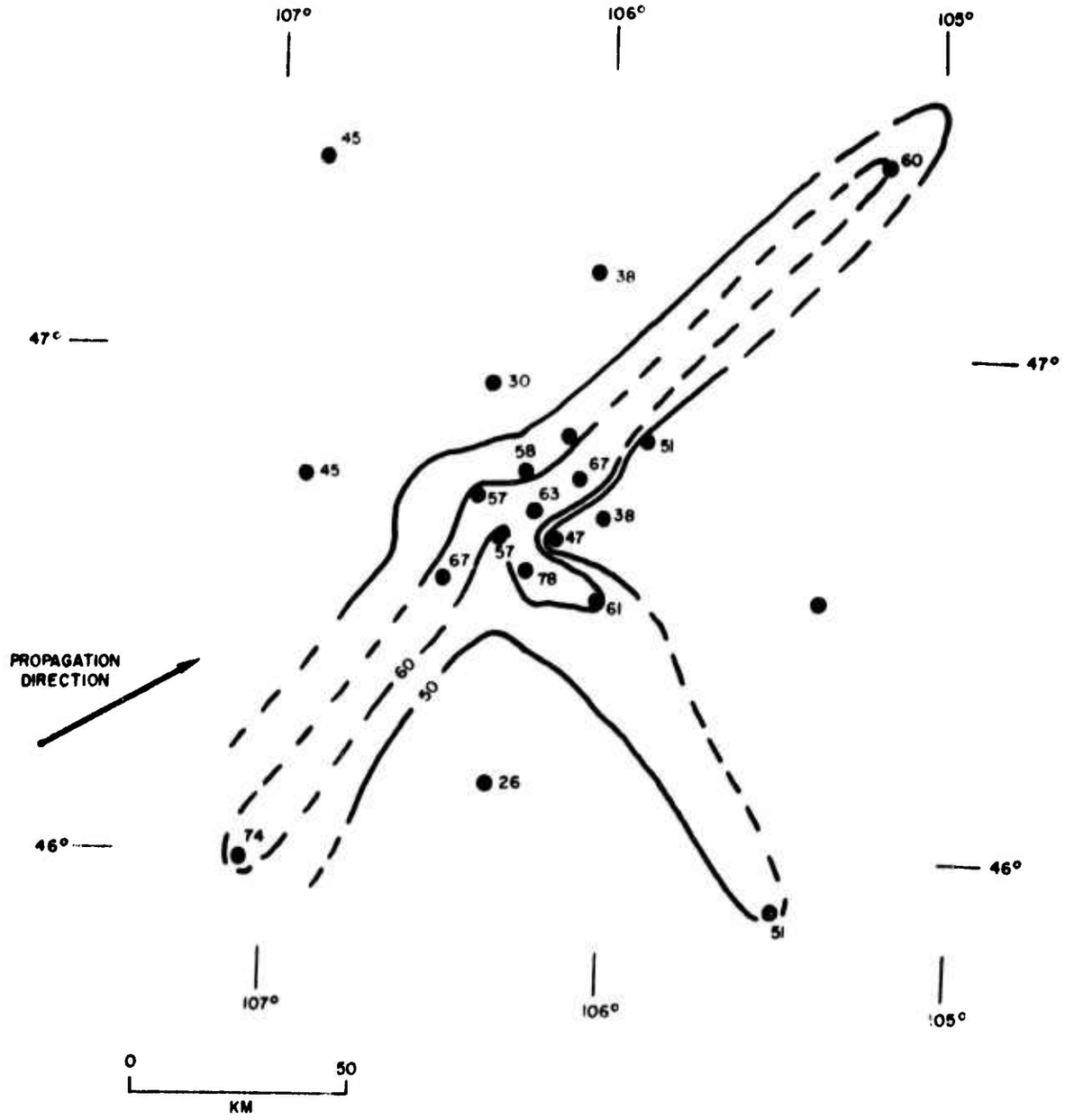

Figure 34. Contour Map Showing (zero-to-peak) P-wave Amplitude Recorded at LASA for the Event 9 December 1965 at 03:35:11.7

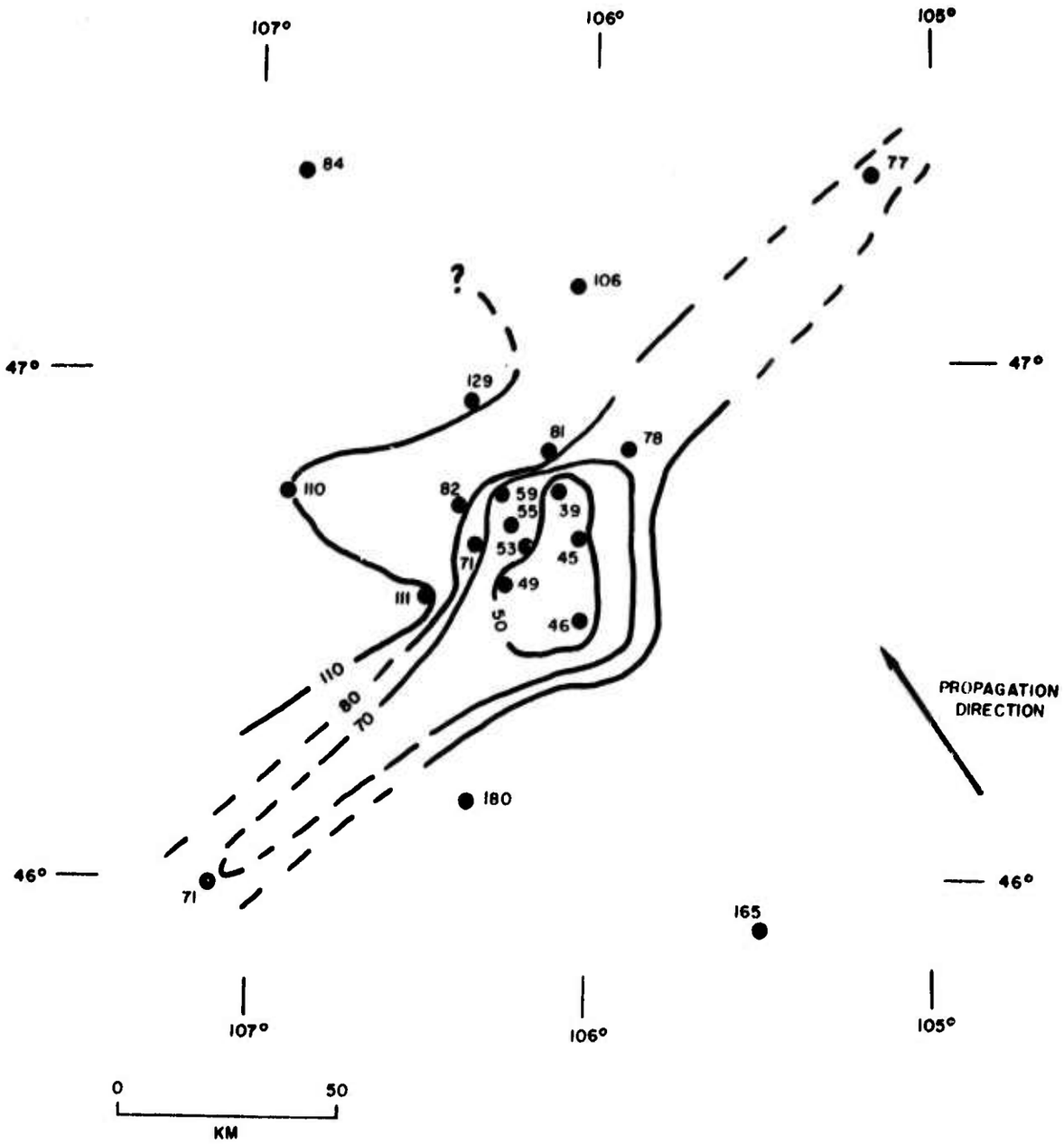

Figure 35. Contour Map Showing (zero-to-peak) P-wave Amplitude Recorded at LASA for the Event 10 November 1965 at 01:47:28.0

component in the geological structure. The other, NE-SW, trend is an important factor contributing to the distribution of travel-time anomalies at LASA and corresponds to trend of the palaeo-structure in the Paleozoic rocks beneath the array. However, the latter trend does not appear as a major factor from the dispersion data.

Any final crustal model for LASA should take into account both these trends.

Gravity Data

A map showing the residual Bouguer gravity anomalies for the State of Montana has been given by Meyer, et al., (1961). The U.S. Geological Survey has recently compiled a detailed map showing the Bouguer anomalies in the immediate vicinity of LASA (Pakiser, personal communication, 1967). The latter shows a closed relative low over the center of the array. To the west of this low there is a relative high which is associated with the Porcupine Dome, and to the south there is another relative high which probably corresponds to the Miles City Arch.

Though the predominant features on the USGS map are the closed lows and highs, there is a suggestion of a deep anomaly trending NW-SE through the center of the array which may correspond to the magnetic boundary postulated by Zeitz. The gravity map of the entire state (Meyer, et al., 1961) shows that the closed features are elongate and orientated with their long axes NW-SE. From this map it can be seen that the regional trend in the vicinity of LASA is from large negative anomalies over the Rocky Mountains in the west to broad, somewhat smaller, negative anomalies over the Great Plains to the east.

Aeromagnetic Data

In the summer of 1966 an aeromagnetic survey was conducted in the vicinity of LASA by the U.S. Geological Survey. A preliminary map of the total magnetic field intensity over the array has been compiled by Zeitz (personal communication, 1967). The map shows several interesting features.

i) To the west of line A-A' (See Figure 1), the isogamma contours are more closely spaced than those to the east.

ii) The western sector of the map shows several very large magnetic anomalies, while to the east the anomalies are much less pronounced.

iii) Projection of the line A-A' to the north and to the south marks the eastern margin of known surface outcrops of igneous rocks (Zeitz, personal communication, 1967), specifically, the Bear Paw Mountains in the north and the Black Hills uplift in the south.

iv) The close correspondence of the anomaly over the Porcupine Dome (see Figure 2 for location) with the depth of the Colorado Shale is in marked contrast with two large anomalies to the south of the array, which have no counterparts in the base of the Colorado Shale. This indicates that the magnetic anomalies while associated with the basement rocks, are not due solely to differences in relief of the latter, but to mafic intrusions within the basement also. Zeitz (personal communication, 1967) believes that the bulk of the crust to the west of the line A-A' is considerably more mafic than the crust to the east.

The trend of the line A-A' is in excellent agreement with the trend of the major structural features as determined from the Rayleigh wave dispersion data. The line A-A' is subparallel to the NW-SE trend of the geologic features and the axes of the major gravity anomalies in Montana.

DISCUSSION

The most striking feature of the evidence presented here is its consistency. The repeated appearance of the NW-SE trend suggests that this is fundamental to the structure beneath the array. Only in the distribution of travel-time anomalies is it not readily discernable. In this section we shall attempt to explain our observations in terms of a model which may form the basis for future investigations.

From the Rayleigh wave dispersion data, supplemented by the evidence from the spectral ratios and the aeromagnetic map, it is evident that as a starting point LASA may be divided into two sectors by the line A-A' (see Figure 1). To the east of this line the observed phase velocities are higher than those to the west. Of the crustal models considered, U.W.3 best fits the observed data for the eastern sector, whereas USGS3 best fits the observed data for the western sector of LASA.

Some important implications of this division are:

i) Seismic velocities in the eastern sector are significantly higher than those in the western sector;

ii) The total thickness of the crust is greater in the east than in the west;

iii) The models indicate a reduction in the number of major layers within the basement, from three in the east to two in the west.

The observed decrease in phase velocities to the west of A-A' is in apparent contradiction to the overall reduction in thickness of the crust inferred from the seismic refraction results. To explain this it is necessary to postulate the presence either of dipping layers within the crust, or lateral changes in velocity within particular layers, or both. Dipping layers have been identified in the seismic refraction studies (See Figures 4 and 5); furthermore, the implied reduction in the number of layers within the basement may be explained in this manner.

The nature of the boundary between the two sectors is problematical. The geologic data do not indicate the presence of large fault or fault zone within the sedimentary sequence (i.e. the uppermost three km) of the crust. This is emphasized by the dispersion results, which indicate that the amount of lateral refraction which Rayleigh waves undergo on crossing LASA increases with depth, at least to about 50 km. This implies that the boundary lies at some depth within the crust, as has been postulated by Zeitz (personal communication, 1967) on the basis of the magnetic data.

Moreover, it is possible that the boundary is gradational rather than abrupt. The dispersion results indicate only that a change takes place. We must await the detailed interpretation of the gravity and magnetic maps before speculating on the nature of the boundary itself.

So far we have sought only to explain the dispersion results. The travel-time anomalies must also be explained in terms of a crustal model. Of the explanations put forward to date, three will be discussed here; bearing in mind that any explanation must satisfactorily account for the "synclinal" feature reported by Sheppard (1967) and substantiated by our results.

To explain the synclinal feature Sheppard (1967) has proposed two alternate hypotheses. They are:

i) A relative thickening of the earth's crust by some 10 km under subarray B4 with respect to F2 and F4. This would correspond to a five- to six-degree slope in the Moho from F4 to F2 and from F2 to B4.

ii) A thickening of the 3.0 km/sec (sedimentary) layer by 3 km under subarray B4.

Neither of these hypotheses are supported by our results. If the Moho dips by as much as 5 degrees then the division of the array into northern and southern sectors should yield relatively lower phase velocities in the north compared to the south, for the Greenland Sea event. As was indicated previously, the phase velocities for the southern sector were higher than those for the northern sector. Also the division of LASA into an inner and outer group of subarrays indicated no strong thickening under the center of the array. From a consideration of the well-log data and from the geologic sections presented by Brown and Poort (1965), there is no evidence to suggest an increase of 3 km (nearly 100%) in the sedimentary sequence anywhere under LASA.

The third hypothesis, proposed by Fairborn (1966), suggests that the azimuthal dependency of the travel-time anomalies requires horizontal velocity gradients in the

crust and upper mantle. Our data and Sheppard's (1967) indicates that horizontal velocity gradients are insufficient in themselves to account for the observed anomalies. Both the seismic refraction data and the Rayleigh wave dispersion data indicate that the average velocity of a 55-km-thick section under LASA decreases from east to west. Such a decrease in velocity would result in systematically later arrivals towards the west of the array if horizontal velocity gradients alone are responsible for the observed travel-time anomalies. From our observations and Sheppard's, the later arrivals define a "synclinal" feature to the NE of A0. This suggests that two of the more important factors bearing on the distribution of the observed travel time anomalies are

i) dipping layers within the crust;

ii) the pre-Cretaceous structure of the Paleozoic rocks and possibly the upper part of the basement also.

Moreover, since large amplitudes are consistently recorded at the center of LASA, it seems that the anticlinal structures which surround the array (see Figure 2) give rise to a lens effect which results in the "focusing" of body waves toward the center of the array. However, more observations are needed to substantiate that this occurs.

CONCLUSIONS AND RECOMMENDATIONS

From the analysis of the geologic and geophysical data presented here we conclude:

1. Lateral variations exist in the structure of the earth's crust beneath LASA. The geologic, aeromagnetic and surface wave dispersion data show that this variation is within the basement at a depth greater than three kilometers. The maximum change takes place in a NE-SW direction (i.e., perpendicular to the dominant NW-SE structural trend).

2. The observations are best explained by dividing LASA into an eastern and a western sector by a line trending N20^{o}W through Miles City, Montana. For the eastern

sector, the average seismic velocities of the crust are higher, the crust is thicker, and Model U.W.3 best accounts for the observed dispersion. For the western sector, the velocities are lower, the crust is thinner, and model USGS3 best accounts for the observed dispersion results.

3. The individual layers within the crust are dipping, though not in the same direction.

In order to further refine the model it is recommended that:

1. The individual travel-time anomalies at each station be obtained as a function of distance and azimuth;

2. More events be examined. In particular, more spectral ratios must be obtained to determine an average structure under each subarray and then Rayleigh waves from events at more azimuths and distances should be analyzed in order to better establish the attitude and thickness of the intermediate crustal layers.

REFERENCES

Aldrich, L.T. and M.A. Tuve, Crustal structure in the Rocky Mountains; Part I: Observation of the University of Wisconsin shots by the Carnegie Institution of Washington, paper presented at the meetings of the IUGG, July, 1960.

Alexander, S.S., Surface wave propagation in the Western United States, Ph.D. thesis, California Institute of Technology, Pasadena, 1963.

Anon., Unpublished company memorandum on LASA, Earth Sciences, Teledyne, Inc., Pasadena, 3 pp., 1965.

Asada, Toshi, and L.T. Aldrich, Seismic observations of explosions in Montana, in The Earth beneath the Continents, Geophys. Monograph 10, edited by J.S. Steinhart and T.J. Smith, pp. 382-390, American Geophysical Union, Washington, D. C., 1967.

Borcherdt, C.A., and J.C. Roller, Preliminary interpretation of a seismic-refraction profile across the Large Aperture Seismic Array, Montana, USGS Tech. Letter No. NCER-2, U. S. Geological Survey, Menlo Park, 31 pp., 1967.

Brown, T.G., and J.M. Poort, Subsurface studies and shallow-hole preparation LASA area, Eastern Montana, Tech, Rep. No. 65-21, The Geotechnical Corp., Garland, 14 pp., 1965.

Brune, J., and J. Dorman, Seismic waves and earth structure in the Canadian Shield, Bull. Seismol. Soc. Am., 53, 167-201, 1963.

Chiburis, E.F., LASA travel-time anomalies for various epicentral regions, Seismic Data Laboratory Report No. 159, 6 pp., 1966.

Cooley, J.W. and J.W. Tukey, An algorithm for the machine calculation of complex Fourier series, Math. Computation, 19, 297-301, 1965.

Evernden, J.F., Direction of approach of Rayleigh waves and related problems, Part I, Bull. Seismol. Soc. Am., 43, 335-374, 1953.

Fairborn, J.W., Station corrections at LASA, AFSOR Contract Report, Department of Geology and Geophysics, Massachusetts Institute of Technology, Cambridge, 16 pp., 1966.

Harkrider, D.G. and D.L. Anderson, Computation of surface wave dispersion for multilayered anisotropic media, Bull. Seismol. Soc. Am., 52, 321-332, 1962.

Haskell, N.A., The dispersion of surface waves on multilayered media, Bull. Seismol. Soc. Am., 43, 17-34, 1953.

James, D.E., and J.S. Steinhart, Structure beneath Continents: A critical review of explosion studies 1960-1965, in The Earth beneath the Continents, Geophys. Monograph 10, edited by J.S. Steinhart and T.J. Smith, pp. 293-333, American Geophysical Union, Washington, D. C., 1967.

Klappenberger, F.A., Spatial correlation of amplitude anomalies, Seismic Data Laboratory Report No. 195, 8 pp., 196[illegible].

McCamay, Keith, and R.P. Meyer, A correlation method of apparent velocity measurement, J. Geophys. Res., 69, 691-699, 1964.

McCowan, D.W., Finite Fourier transform theory and its application to the computation of convolutions, correlations, and spectra, Seismic Data Laboratory Report No. 168 (Revised), 16 pp., 1967.

McCowan, D.W., Design and evaluation of certain multichannel filters, Seismic Data Laboratory Report No. 204, 17 pp., 1968.

Meyer, R.P., J.S. Steinhart, and W.E. Bonini, Montana, 1959, in Explosion studies of Continental structure, Pubilication No. 622, edited by J.S. Steinhart and R.P. Meyer, pp. 305-343, Carnegie Institution of Washington, Washington, D. C., 1961.

Miller, M.K., A.F. Linville, and H.K. Harris, Continuation of basic research in crustal studies, Final Report AFSOR 67-1581, Texas Instruments, Inc., Dallas, 116 pp., 1967.

Phinney, R.A., Structure of the Earth's crust from spectral behavior of long-period body waves, J. Geophys. Res., 69, 2997-3017, 1964.

Sheppard, R.M., Values of LASA time station residuals, velocity and azimuth errors, Technical Note 1967-44, Lincoln Laboratory, Massachusetts Institute of Technology, Lexington, 95 pp., 1967.

Smith, J.G., Fundamental transcurrent faulting in Northern Rocky Mountains, A.A.P.G. Bull., 49, 1398-1409, 1965.

Steinhart, J.S., and G.P. Woollard, Seismic evidence concerning continental crustal structure, Explosion studies of Continental Structure, Publication No. 622, edited by J.S. Steinhart and R.P. Meyer, pp. 345-383, Carnegie Institution of Washington, Washington, D. C., 1961.

Stoneley, R., On the apparent velocity of earthquake waves over the surface of the earth, Mon. Nat. Roy. Astron. Soc. Geophys. Suppl., 3, 262-271, 1935.

APPENDIX I

EXPERIMENTAL MEASUREMENT OF PHASE VELOCITY DISPERSION

THEORY:

The travel-time of a given period T between stations may be written (Alexander, 1963) as

$$\delta t_{ij} = t_i - t_j + T \left[\phi_j(T) - \phi_i(T) \pm N_{ij} \right] \qquad (1)$$

where t_i = the time (with respect to some standard common to all stations) of the first digital sample at the i^{th} station.

t_j = the time (with respect to the same standard as t_i) of the first digital sample at the j^{th} station,

$\phi_i(T)$ = observed phase (fraction of a circle) with respect to t_i at the i^{th} station minus the instrument phase for period T at the i^{th} station,

$\phi_j(T)$ = observed phase (fraction of a circle) with respect to t_j at the j^{th} station minus the instrument phase for period T at the j^{th} station,

and N_{ij} = arbitrary integer, which must be determined.

Taking the i^{th} station as the psuedo-origin (i.e. setting the arrival time of the k^{th} period T_k at the i^{th} station equal to zero), δt_{ij} becomes the relative arrival time of the k^{th} period at the j^{th} station,

$$\tau_{jk} = \Delta_j \cos \alpha_j \cos \theta_k / C_k + \Delta_j \sin \alpha_j \sin \theta_k / C_k + \tau_{ik} \qquad (2)$$

where Δ_j = distance of the j^{th} station from the psuedo-origin α_j = azimuth of the j^{th} station from the psuedo-origin

θ_k = direction of propagation of k^{th} period across the array and C_k = phase velocity of k^{th} period across the array then

$$\tau_{jk} = a_j x + b_j y + z \qquad (3)$$

where

$x = \cos \theta_k/C_k$, $y = \sin \theta_k/C_k$ and z = predicted time at pseudo-origin,

which may be solved in least-squares sense to give $\hat{x}$, $\hat{y}$, $\hat{z}$, and $\sigma_{\hat{x}}$, $\sigma_{\hat{y}}$, $\sigma_{\hat{z}}$.

Then

$$\theta_k = \tan^{-1} (\hat{y}/\hat{x}), \quad C_k = (\hat{x}^2 + \hat{y}^2)^{-\frac{1}{2}}$$

The standard deviations of θ_k and C_k may then be found from the well-known relationship

$$\sigma_\gamma = \left[\sum_j (\sigma_{\mu_j} \partial\gamma/\partial\mu_j)^2 \right]^{\frac{1}{2}}$$

where

$$\gamma(\mu_1, \mu_2 \ldots \mu_j) \equiv \gamma\ (x,y,z)$$

Method of Analysis

A FORTRAN63 program was written for the CDC 1604 computer to implement the procedure outlined above. Filtered digital seismograms, with a sampling rate of 0.5 points per second were input from tape for each station. Phase arrival times relative to the reference station were determined from the phase of the Fourier transform of the record computed using the Cooley-Tukey algorithm (Cooley and Tukey, 1965). The integer N_{ij} was determined by inspection form these phase arrival times. If the absolute value of the phase arrival time at period T for a given station exceeded nT seconds, where n is an integer, then the $|N_{ij}|$ was set to n and the sign of N_{ij} adjusted such that stations nearer the source than the reference recorded earlier arrival times and more distant stations later arrival times.

The distances and azimuths from the reference station to the remaining stations were input from cards. From the relative arrival times and station locations, a least-squares error estimate

of the phase velocities and propagation directions over a specified period range was found. The actual interval of period at which the phase velocities were calculated is predetermined by the transform algorithm and is a function of the seismogram length and sampling rate (see McGowan, 1967).

The phase velocities found using this program scattered quite badly, particularly at the longer periods. In order to smooth the dispersion curves, the relative phase arrival times were fitted by least-squares to a polynomial in frequency. Since the interval at which these times are determined is non-uniform with period, each relative arrival time was given weight equal to the magnitude of the corresponding period to avoid biasing the points at the higher frequencies where determinations of arrival time are more frequent. These fitted times were then used in the velocity determinations.

It was found that a linear fit was adequate, and all subsequent phase velocity dispersion curves were obtained in this manner.

Experimental Measurement of Group Velocity Dispersion

A by-proudct of the modified phase velocity dispersion program is a polynomial giving relative phase arrival times for each station as a function of frequency. This polynomial can be used to obtain the group velocity

$$U_k = U(T_k)$$

using an expression analogous to equation (2),

$$(\phi_j - \phi_i)'_k = \Delta_j \cos \alpha_j \cos \theta_k/U_k + \Delta_j \sin \alpha_j \sin \theta_k/U_k + \tau_{ik} \qquad (4)$$

where

$(\phi_j - \phi_i)'_k$ = deviative with respect to frequency (Hz) of the phase difference between the j^{th} station and the reference station evaluated at the period T_k

τ_{ik} = predicted group arrival time at the reference station (previously this denoted the predicted phase arrival time in equation 2)

θ_k = group propagation direction for the period T_k

Δ_j, α_j = same as in equation (2).

We evaluate the derivative of the polynomial at specified periods and input the relative group arrival times $(\phi_j - \phi_{i_k})'$ to the velocity-calculating subroutine and thus obtain the group velocity dispersion curves.

APPENDIX II

CALCULATION OF THE TREND OF THE BOUNDARY BETWEEN THE EASTERN AND WESTERN SECTORS OF THE ARRAY.

Surface waves obliquely incident on a boundary separating regions of different velocity structure are laterally refracted in a manner governed by the phase velocities in the two regions (Stonely, 1934, Evernden, 1954). In the case where the boundary is linear and the equicentral distance is sufficiently great that the wave-fronts may be considered plane, the following relationship (Snell's law) holds:

$$\frac{\sin i_2}{C_1(T)} = \frac{\sin i_2}{C_2(T)}$$

where i_1 = angle of incidence that a given surface wave makes with the boundary measured in region 1, i_2 = angle of incidence that the same wave makes with the boundary in region 2, $C_1(T)$ = phase velocity in region 1, $C_2(T)$ = phase velocity in region 2, and T = period. This relationship enables us to determine the strike of the boundary from the measured propagation directions in the two regions (Alexander 1963).

Since the angles i_1 and i_2 are initially unknown, only the difference in propagation direction $\beta_i(T)$ of a given phase between the two sectors can be determined (See Figure II-1). However, by plotting $\alpha_i(T)$ the back azimuth to the apparent source vs. $\beta_i(T)$ for serveral events, it is possible to determine the intercept which the curve makes with the α- axis, $\alpha_o(T)$. $\alpha_o(T)$ then is the direction exactly normal to the boundary between the two regions. The strike of the boundary θ, measured counter-clockwise from North, is simply $(90 - \alpha_o)$ degrees.

Only two events were available, in the present analysis, from which to calculate the strike of the boundary between the eastern and western sectors of the array, as defined above. The propagation

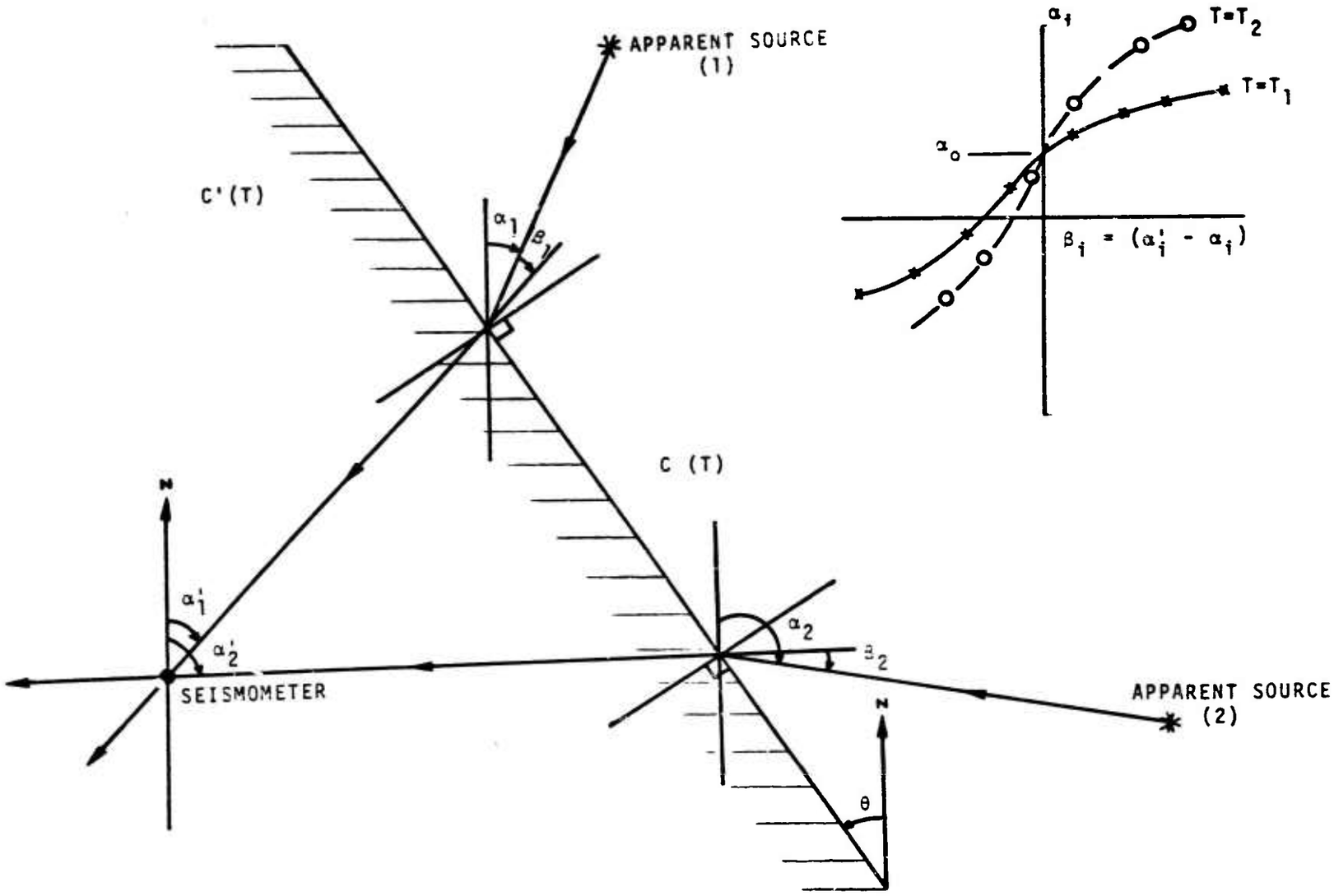

Figure II-1. Method of Determining the Strike of the Boundary Separating Two Regions of Contrasting Phase Velocities

directions in the eastern sector of LASA minus 180 degrees define $\alpha_i(T)$. This eliminates refraction effects between the actual source and the perimeter of the array. The difference in propagation direction of a given phase between the western and eastern sector gives $\beta_i(T)$. Since there are but two points to define the curve α vs β, at a given period T we are forced to approximate it with a straight line. Thus the intercept of the curve with the α-axis places a lower bound on α_o.

Unclassified

Security Classification

DOCUMENT CONTROL DATA - R&D

(Security classification of title, body of abstract and indexing annotation must be entered when the overall report is classified)

1. ORIGINATING ACTIVITY (Corporate author)
TELEDYNE, INC.
ALEXANDRIA, VIRGINIA 22314

2a. REPORT SECURITY CLASSIFICATION
Unclassified

2b. GROUP

3. REPORT TITLE
LATERAL VARIATIONS IN CRUSTAL STRUCTURE BENEATH THE MONTANA LASA

4. DESCRIPTIVE NOTES (Type of report and inclusive dates)

5. AUTHOR(S) (Last name, first name, initial)
Glover, P., Alexander, S.

6. REPORT DATE	7a. TOTAL NO. OF PAGES	7b. NO. OF REFS
16 February 1968	63	25

8a. CONTRACT OR GRANT NO.	9a. ORIGINATOR'S REPORT NUMBER(S)
F 33657-67-C-1313 b. PROJECT NO. VELA T/6702 c. ARPA Order 624 d. ARPA Program Code No. 5810	205 9b. OTHER REPORT NO(S) (Any other numbers that may be assigned this report)

10. AVAILABILITY/LIMITATION NOTICES
This document is subject to special export controls and each transmittal to foreign governments or foreign national may be made only with prior approval of Chief, AFTAC

11. SUPPLEMENTARY NOTES	12. SPONSORING MILITARY ACTIVITY
	ADVANCED RESEARCH PROJECTS AGENCY NUCLEAR TEST DETECTION OFFICE WASHINGTON, D.C.

13. ABSTRACT

The analysis of a variety of geologic and geophysical data indicates that signigicant lateral variations in crustal structure exist across LASA. This structural complexity is inferred from observation of Rayleigh wave dispersion, body-wave spectral ratios, P-wave amplitude and travel-time anomalies, seismic refraction profiles and gravity and magnetic anomalies. To explain these results, LASA is divided into an eastern and a western sector. An attempt is made to explain the observations in each sector in terms of crustal models consisting of 3 to 5 distinct layers. The observations show that the maximum lateral change in structure across LASA takes place in a NE-SW direction.

14. KEY WORDS

LASA, structural complexity, lateral variations, dipping layers, crustal thickness, eastern sector, western sector, crustal models.

Unclassified

Security Classification